Using Thermographic Image Analysis in Detection of Canine Anterior Cruciate Ligament Rupture Disease

by Jiyuan Fu, Bachelor of Science

A Thesis Submitted in Partial
Fulfillment of the Requirements
for the Degree of Master of Science
in the field of Electrical and Computer Engineering

Advisory Committee:

Scott E Umbaugh ,Chair

Brad Noble

Robert LeAnder

Graduate School
Southern Illinois University Edwardsville
December, 2014

ProQuest LLC.
789 East Eisenhower Parkway
P.O. Box 1346
Ann Arbor, MI 48106 - 1346

ABSTRACT

USING THERMOGRAPHIC IMAGE ANALYSIS IN DETECTION OF CANINE ANTERIOR CRUCIATE LIGAMENT RUPTURE DISEASE

by

JIYUAN FU

Chairperson: Professor Scott E Umbaugh

Introduction: Anterior cruciate ligament (ACL) rupture is a common trauma which frequently happens in overweight dogs. Veterinarians use MRI (Magnetic resonance imaging) as the standard method to diagnose this disease. However MRI is expensive and time-consuming. Therefore, it is necessary to find an alternative diagnostic method. In this research, thermographic images are utilized as a prescreening tools for the detection of ACL rupture disease. Additionally, a quantitative comparison is made of new feature vectors based on Gabor filters with different frequencies and orientations.

Objectives: The main purpose of the research study is to investigate whether thermographic imaging can be used effectively in canine ruptured anterior cruciate ligament (ACL) disease detection. And to determine whether using the **Gabor Filter** with different frequencies and orientations for the new feature extraction can improve the result.

Methods: The mask made manually will be used for focusing on the region of interest (ROI).For the canine anterior cruciate ligament ruptures investigation, four color normalization methods are implemented on each category based on three different views: anterior, lateral, posterior. Histogram, texture and spectral features are extracted by CVIP-

FEPC. After these twelve filters being convolved with the thermographic image, the new feature vectors are used for pattern classification.

Results: When using first/second order histogram features, the best classification rate of anterior view is 83.93% which is produced by the NormGrey images. The best classification rate of lateral view is 83.93% which is from NormGrey and NormRGB images. The best classification rate of posterior view is 82.14% which is from NormRGB-lum images. Using the Gabor filter based features for the anterior, lateral and posterior view images, the best classification success rate 87.50%, 83.93%, 85.71% was achieved respectively. Comparing to results using the first/second order histogram features, the best classification rates using Gabor filter increased from 0.00% to 3.57%.

Conclusion: It is possible to detect the canine Anterior Cruciate ligament (ACL) ruptures with thermographic images. Also images with Gabor filter processing which involve frequency and orientation information provide a small improvement in the best success rate.

ACKNOWLEDGEMENTS

First and foremost I would like to express my great appreciation to my advisor, Dr. Scott Umbaugh, for all his generous and professional support and guidance during my master's study. I am very grateful for what he has done for me. I am lucky and also proud of being a student of his.

Also,I am very thankful to my advisory committee members, Dr. Brad Noble and Dr. Robert LeAnder, for their help and patience.

Besides, I want to provide my true gratitude to my fellow group members, Samrat Subedi, Ravneet Kaur, Krishna Regmi, Heema Poudel and Hari Bhogala for their great help. Also I would like to thank Dr. Dominic J. Marino and Dr. Catherine A. Loughin from Long Island Veterinary Specialists [LIVS] for providing funding and help for this research.

Last but not the least I would like to thank my whole family for their love and encouragement.

TABLE OF CONTENTS

LIST OF FIGURES

Figure Page

LIST OF TABLES

Table Page

CHAPTER 1

INTRODUCTION

Ligaments are injury prone for both humans and animals. When the anterior cruciate ligament (ACL) ruptures, the ligament may become malpositioned. Also, sports might cause second-time injury to the ACL. Each year, the incidence rate of ACL rupture disease appears to be increasing and therefore exploring an efficient method to detect ACL rupture is necessary. For current methodology, ultrasonography, x-ray, computed tomography (CT) and magnetic resonance imaging (MRI) diagnostic methods are commonly utilized for detection of the diseases. Comparing with others, the MRI is the optimal method. But, it is costly and time consuming. Additionally, it is quite difficult for an injured dog to remain in the same position for the long time required for the MRI and the radiation exposure can be harmful. To reduce the overall cost and save time, the goal of this research study is to investigate the efficacy of the thermographic imaging diagnostic method for canine ruptured cruciate ligament detection.

This research utilizes of computer imaging processing and pattern recognition techniques in detection of canine ACL rapture disease. Those thermographic images taken under the infrared camera from Long Island Veterinary Specialists (LIVS) are divided into *normal, or healthy* and *abnormal*, *or injured* categories. According to different camera views, these thermographic images are also divided into contralateral anterior, lateral and posterior views.

In general, images contain a huge amount of data. Image processing and computer vision techniques are used to extract pertinent features to minimize the redundant information. Feature extraction is used convert the image data into a feature space. The feature space is established with different combinations of the features, which are automatically extracted using CVIP-FEPC. Finally, these features vectors are utilized for pattern classification.

Also, to improve the possibility to achieve the goal, the Gabor filters are utilized in this research to compare with the first/second order histogram feature measurements The Gabor filter is a linear filter which is appropriate for texture segmentation and discrimination, and is used here to generate new features.

1.1 Objectives of the Thesis

The main purpose of the research study is to investigate whether thermographic imaging can be used effectively in canine ruptured anterior cruciate ligament (ACL) disease detection. The objectives of this research are shown as follows:

- Determine the efficacy of using thermographic images to classify canine ACL rupture disease
- Implement Gabor filter with different frequencies and orientations.
- Classify the images by using first/second order histogram feature measurement and new feature measurements which involve the Gabor filter.
- Determine the best combination of features for first/second order histogram feature measurement and best orientation and frequency for Gabor filter feature measurement.

- Make a comparison of result between standard texture features based on histograms to Gabor filter features.
- Analyze and compare results for different camera views
- Analyze and compare results for different color normalization methods

1.2 Outline of the Thesis

As follows:

Chapter 1 concisely introduce what in this research.

Chapter 2 presents background and literature review of this study, the technique of infrared imaging and the Gabor filter.

Chapter 3 provides a brief introduction of the materials and software used in this research.

Chapter 4 presents the specific processing for experiments. Four main processes are involved: border mask creation, color normalization, feature extraction, pattern classification. Also, the Gabor filter implementation is discussed.

Chapter 5 discusses and analysis the results of first/second order histogram feature measurement and Gabor filter feature measurement.

Chapter 6 summarizes the results and conclusion of experiments.

Chapter 7 shows the future outlook of this study.

CHAPTER 2

LITERATURE REVIEW

Diagnostic imaging is a process for acquiring visual representations of the human or animals' body for medical analysis and research. It seeks to reveal internal structures hidden by the skin and bones [Nick; 2014]. Therefore the diagnostic method is an extremely important part of diagnosing the diseases and determining treatment of diseases. The aim of this paper is to compare different feature extraction methods while diagnosing diseases with thermographic images. The object of this chapter is to provide some relevant arguments and background knowledge. This section contains three categories:1) Background, 2) Infrared thermographic image and image processing technique, 3) Gabor Filter technique.

2.1 Background

Anterior cruciate ligament (ACL) rupture is a common trauma for canine. The anterior cruciate ligament controls rotational movement and prevents forward movement of the tibia in relation to the femur [Hyalay; 2012].When bruised, the ligament may become malpositioned or ruptured injuries can occur anytime even within normal activity levels. It happens often in overweight canines, because obesity provides more pressure to the ligament [Foster; 2010]. A variety of diagnostic methods have been widely used in detection of the disease .Typically it is required to scan through the body of patients. This technique can be helpful for the physician to determine the position of the injury. Diversified diagnostic methods can be used for different cases.

Currently，diagnostic methods may vary depending on different diseases. Ultrasonography, x-ray, computed tomography (CT) and magnetic resonance imaging (MRI) diagnostic methods are typical methods for disease detection. Most of methods are painful and time consuming [Freddie;2008]. Additionally, some methods are invasive which may be harmful to patients. Among these methods, the MRI imaging method is considered as the most optimal method. Magnetic resonance imaging (MRI) can detect the internal organs by scanning the body with magnetic waves. MRI is excellent for physical examination. Comparing with CT and other diagnostic methods, MRI offers high-level resolution and is noninvasive [Naranje; 2008][Huysse,;2008] It is required that patients or animals be keep motionless under the magnetic scanning in this case. Meanwhile, it is very difficult for dogs to maintain the same posture for a long time and it may be harmful to them to stand long in strong radiation. Also, MRI is an expensive and complex diagnostic method. While MRI has its benefits, it is potentially beneficial to find a new alternative diagnostic method. To reduce the cost and save time, the infrared thermographic image technique is used for this research for canine ACL injury disease detection.

2.2 The Infrared Thermographic Image and Image Processing Technique

Digital Infrared Thermal Imaging (DITI) is a noninvasive diagnostic method which has been widely used in the medical field. In this section, the background of infrared thermographic technique and image processing technique are discussed.

2.2.1 The infrared thermographic technique

The infrared thermography technique (IRT) makes it possible to observe thermal information by transferring heat data which is emitted from objects into a visible

thermographic image. All objects with temperatures above absolute zero emit heat, which makes the information collectable by thermography equipment [Azmat; 2005]. Infrared thermography transfers light radiation into the IR region, therefore accurately measures the intensity of thermal radiation with different wavelengths [Barr; 1965]. Warm-blooded creatures become visible against the environment with a thermal imaging camera because warm objects and cooler backgrounds offer different temperature distributions. As a consequence, the infrared thermography technique is of great use and importance for medical science and military applications [Lisowska-Lis; 2011].

In an attempt to detect the pathological condition of canines with ruptured anterior cruciate ligaments, thermographic images taken with the infrared camera by the Long Island Veterinary Specialists (LIVS) will be classified into normal and abnormal categories. All dogs in the normal category have had a physical exam and diagnostic x-rays to confirm that there are no orthopedic issues currently or in the past. All dogs in the abnormal category have had an examination, x-rays, and corresponding surgery confirming that the cruciate ligament of the lame leg is "torn" and the opposite leg is considered normal [LIVS; 2013].

To obtain more information for the distribution of temperature, these thermographic images are taken with three different views: anterior, lateral, posterior view. Anterior, lateral, posterior views are referring to taking images from front, side and back of the animal respectively.

2.2.2 Image processing technique

In this research, the thermographic images from LIVS will be classified by using computer vision and image processing techniques. These images need to be analyzed by simplifying the raw image data into higher level information which involves a dimensional

reduction. The process of transforming the row image data to the set of features is known as feature extraction.

After the features are extracted from all images, a combination of pattern classification methods selected by the user is implemented. To explore more features for detection, the Gabor filter is used.

2.3 Gabor Filter

The Gabor filter, is a linear filter which has been utilized effectively for edge detection. It is characterized by frequency and orientation. Because of the attribution, it has been regarded to be suitable for texture segmentation and discrimination [Kruizinga ;1999]. In the spatial domain, a 2D Gabor filter is the result of multiplication of a 2D Gaussian function and an exponential function, which can be represented as follow:

$$g(\lambda, \theta, \varphi, \sigma, \gamma) = \exp(-\frac{x(\theta)^2+\gamma^2 y(\theta)^2}{2\sigma^2})\exp(i(2\pi\frac{x(\theta)}{\lambda} + \varphi))$$

Details of the Gabor filter will be explained in Chapter 4.

A set of Gabor filters with several frequencies and orientations may be helpful for extracting useful features from images. Therefore Gabor filters have been widely used in pattern classification applications. Many applications have used the Gabor filter effectively, such as face recognition and fingerprint recognition.

According to previous research, the Gabor features are extracted from human faces, then slow feature analysis (SFL) is applied which was effectively used for face recognition [Gao et al; 2008]. Also, another application extracted the local Gabor features including eyes, nose, ears and lib with eight different angles and five different frequencies. Then they mark common points and calculate the distance between them. Finally, these distances are

compared with database. If match occurs, the images are successfully recognized [Muhammad et al; 2011].

There are some application that use Gabor filter for fingerprint recognition. The fingerprint images were separated into sets of 32*32 small subimages. They used Gabor filter-based features vectors which are directly extracted from grey-level subimages, as new feature vectors to a nearest neighbor and k-nearest neighbor (K=2,3) classifier to compare with a fingerprint database. The result shows an improvement by using the convolved Gabor filter [Lee et al; 1999].

Both face and fingerprint recognition can be improved by convolving the Gabor filter at different scales. Therefore, the Gabor filter can be utilized as a texture mask for enhancing the orientation and frequency data which is beneficial for pattern classification. Gabor features can be used directly as input to a classification or segmentation operator or they can be firstly transformed into new features which are which are then used as such an input [Grigorescu; 2002]. In this research, the Gabor filters are implemented with three different frequencies and four different orientations. After these twelve filters are applied to the thermographic images, the Gabor feature vectors are used for pattern classification. The Gabor feature vectors are obtained by extracting the standard first and second order histogram/texture features from the Gabor images themselves One goal of the research study is reached to investigate whether the Gabor filter can improve the efficiency of anterior cruciate ligament (ACL) disease detection.

CHAPTER 3

MATERIALS AND TOOLS

The main purpose of the research study is to investigate whether thermographic imaging can be used effectively in canine ruptured anterior cruciate ligament (ACL) disease detection. The materials utilized in this research include thermographic images from the Long Island Veterinary Specialists and border masks created in the Computer Vision and Image Processing (CVIP) research lab at SIUE. There are five main programs involved: CVIPtools, CVIP-FEPC, Matlab, Color Normalization software, and Microsoft Excel.

3.1 The Thermographic Images

In this research, a digital infrared thermal imaging (DITI) system from Meditherm Med2000 IRIS is used. It is provided by the Long Island Veterinary Specialists (LIVS). The med2000™ incorporates all of the necessary criteria required for successful clinical digital infrared thermal imaging (DITI). It offers accurate measurement and has the ability to statistically analyze the thermograms at a later date which is very important in clinical work [Meditherm; 2012].

The med2000™ has two parts, the IR camera and a standard PC or laptop computer, making the system very portable.With a high-resolution display, the system can measure temperatures ranging from 10° C - 55° C to an accuracy of 0.01° C. Focus adjustment covers small areas down to 75 x 75mm [Meditherm; 2012].

Thermograms produced by the med2000™ are stored as TIFF RGB images with 319 columns by 238 rows, 8-bits per pixel per color band. The images used in this research are

supplied by Long Island Veterinary Specialists. A total of 18 colors are used in these images [LIVS;2012].

In this research study, as many as twenty-eight dogs with two different groups are used: 1) fourteen normal canines 2) fourteen abnormal canines. In the normal group, both sides of the canines are normal. In the abnormal group, canines have ACL issue with only one limb.

A total of 168 thermographic images are separated into three groups based on these different views: 1) anterior view, 2) lateral view, 3) posterior view. Each group has 56 images. All images can also be categorized into two classes: 1) limbs with ruptured anterior cruciate ligament (ACL) disease, 2) limbs without disease. The number of images in each category is shown in Table 3.1. Examples of the thermographic images of a healthy canine (*normal*) and of a canine diagnosed with ACL disease (*abnormal*) with different views are shown in Figure 3.1, Figure 3.2 and in Figure 3.3 respectively

Table 3.1 The Number of Thermographic Images in Each Category

Pathology	The Number of Images		
	Anterior	Lateral	Posterior
Healthy	42	42	42
ACL rupture	14	14	14

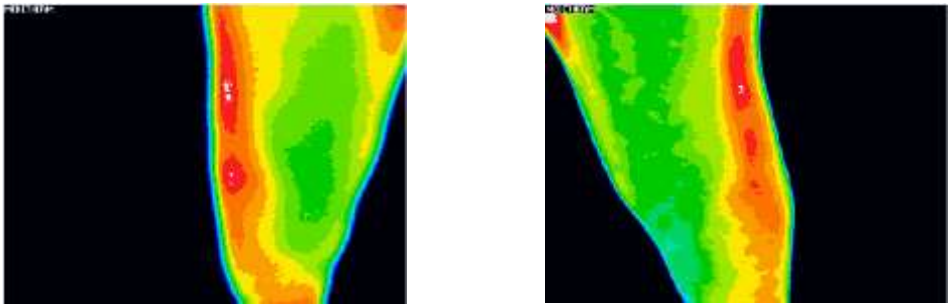

(a) Normal thermal image **(b) Abnormal thermal image**

Figure 3.1 Thermographic Images of a Canine with Anterior View

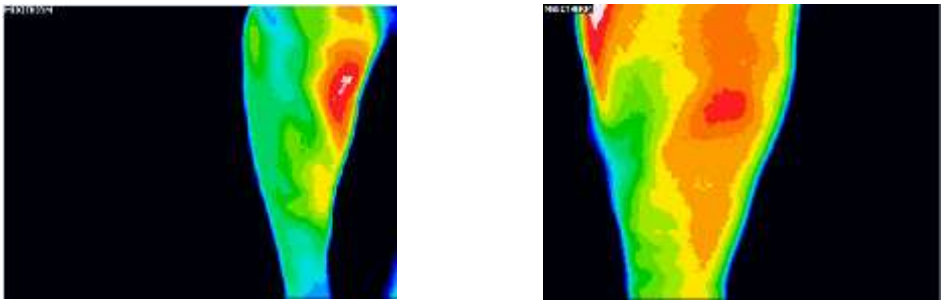

(a) Normal thermal image **(b) Abnormal thermal image**

Figure 3.2 Thermographic Images of a Canine with Lateral View

(a) Normal thermal image **(b) Abnormal thermal image**

Figure 3.3 Thermographic Images of a Canine with Posterior View

3.2 Border Masks

An image may be considered to contain many sub-images. To maintain high accuracy and eliminate the noise and error, extracting the region of interest (ROI) is helpful for focusing on the area under consideration. Border masks are used to extract the ROI with white being the object and black being the background. The ACL disease area is considered the region of interest which is determined by experts from the Long Island Veterinary Specialists (LIVS). Manually border masks creation is implemented in CVIPtools, with *Utilities->Create->Border mask*.

3.3 Software Tools

In this research, the main processing can be categorized in two areas: feature extraction and pattern classification. There are six primary programs utilized for achieving the goal: CVIPtools, CVIP-FEPC, Matlab, Color Normalization software, Partek and Microsoft Excel.

3.3.1 CVIPtools v5.5d

CVIPtools is a Windows-based software which was developed by the Computer Vision and Image Processing (CVIP) Laboratory in the Department of Electrical and Computer Engineering of Southern Illinois University Edwardsville (SIUE). CVIPtools is created to facilitate the development of both human and computer vision applications. This software provides an environment for the user to implement different functions and instantly get the results [CVIPtools; 2012]. CVIPtools version 5.5d is the newest version. In this research, CVIPtools is utilized for manual mask creation. In addition, it is also efficient for comparison of two different images.

3.3.2 CVIP-FEPC (Feature Extraction and Pattern Classification)

CVIP-FEPC [CVIP-FEPC; 2010] allows users to perform feature extraction and pattern classification experiments with one program running. This software will automatically extract all combinations of features based on user selection. It will then perform each pattern classification combination on these features. Finally, the application produces the success rate for the different feature combinations which allows the user to easily find the optimal feature and classification combinations. In addition, sensitivity and specificity metrics are provided in the result which indicates the accuracy of our prediction of disease and absence of disease.

3.3.3 Matlab v2013a

Matlab is a high-level language and interactive environment for numerical computation, visualization, and programming. Matlab provides functions through which the user can analyze data, develop algorithms, and create models and applications [Matlab; 2013].In this research, Matlab is used for implementing the code of the Gabor filter.

3.3.4 Color normalization software

The color normalization algorithm normalizes the original thermographic image into four different color space based on different temperature distribution. These four spaces refer to as luminance (lum), normalized grey (normGrey), normalized RGB (normRGB), and normalized RGB luminance (normRGB-lum) [Umbaugh, Solt; Jan 2008]. These temperature data is provided by the Long Island Veterinary Specialists.

3.3.5 Microsoft Excel

Microsoft Excel is a spreadsheet application for data collection and calculation. In this research, Excel is utilized for result collection and data sorting.

CHAPTER 4

METHODS AND EXPERIMENTS

In this study, there are a total of four steps for ACL disease diagnosis, including:

- Border Mask creation
- Color Normalization
- Feature Extraction
- Pattern Classification

4.1 Border Masks

To eliminate unnecessary image data and focus on the disease area, the border mask operation was used to create the border mask. The border mask image is a binary image. Figure 4.1 shows a ROI with their corresponding original image as provided by LIVS. Figure 4.2 shows images of anterior, lateral and posterior views with their created manually corresponding masks, and the results after application of the mask to extract the ROI. The masked image is the image after “And” operation between original image and mask.

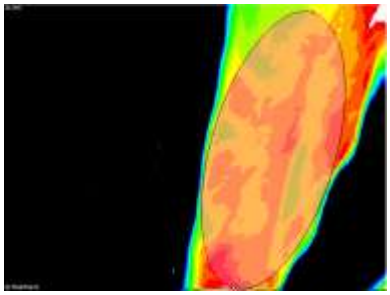

(a) region of interest(ROI) area

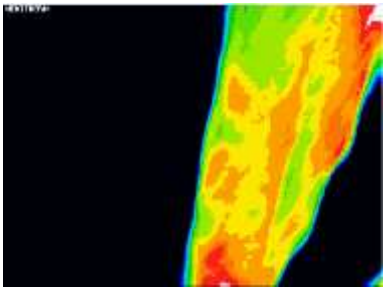

(b) original image

Figure 4.1 Region of Interest to Detect ACL Disease and Original Image

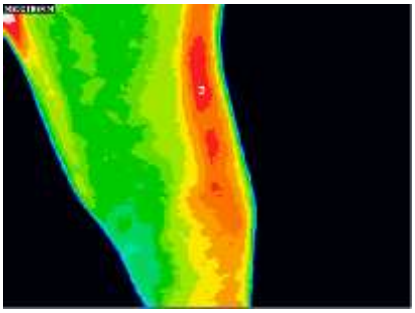

(a) anterior view original image

(b) anterior view mask image

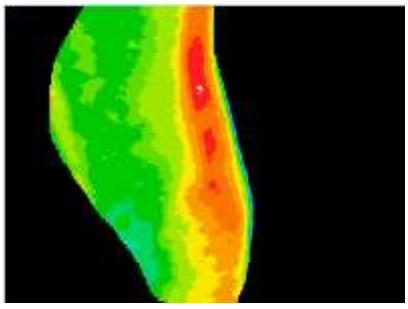

(c)anterior view masked image

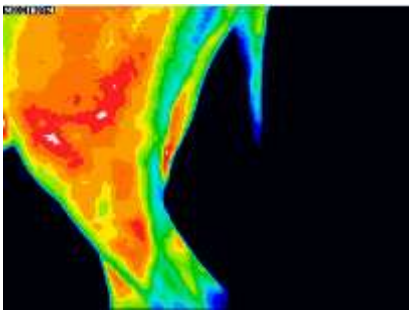

(d) lateral view original image

(e) lateral view mask image

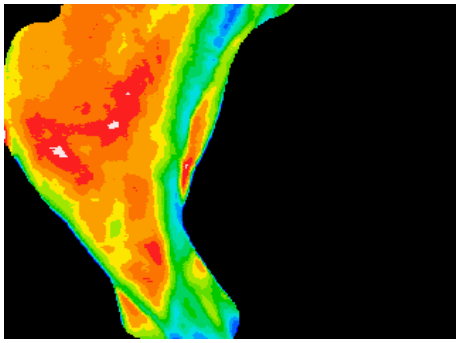

(f) lateral view masked image

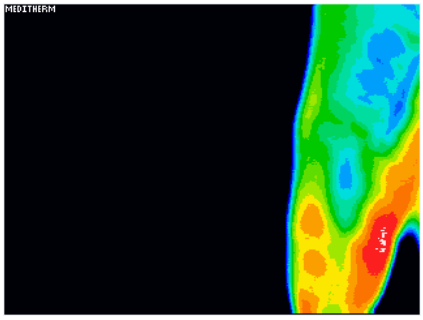

(g) posterior view original image

(h) posterior view mask image

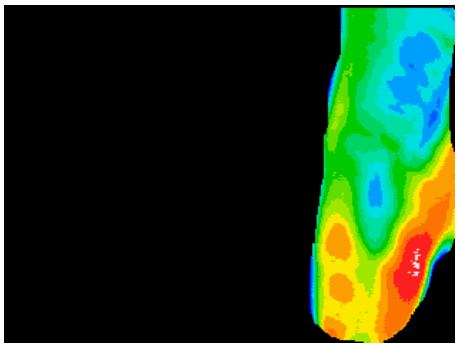

(i) posterior view original image

Figure 4.2 Manual Masks Created from Anterior, Lateral and Posterior View.

4.2 Color Normalization

The distribution of color data in the image depends on illumination, the thermographic data, and the settings of the image acquisition system. In this study, each of the images uses the same color palette consisting of 18 colors. Every color represents a specific temperature value. Since the camera may be recalibrated between each image capture, within a set of images one color may map to several different temperatures. For this study each class, normal and abnormal, was color normalized separately (note that combined color normalization results are in Appendix I). In order to remap the temperature to a common (normalized) temperature scale, four different color normalization methods are used including: Luminance, Norm-Gray, Norm-RGB, Norm-RGB-Lum [Umbaugh, Solt, 2008].

Luminance: Each pixel in the normalized image generates the gray value level follow by the formula:

$$GrayLevel = 0.3 * \text{Red} + 0.6 * Green + 0.1 * Blue$$

[C.A. Loughin et al, Oct 2007]

Which Red, Green, Blue is the value with three bands of RGB color model.

Norm-Gray: Each of the images with same color palette consists 18 colors. Temperatures base on this18 colors from minimum to maximum are remapped from 0 to 255.

Norm-RGB: Norm-RGB method is similar with Norm-Gray while instead of temperatures being remapped to gray level from 0 to 255. They are mapped to a continuous version of the original color palette.

Norm-RGB-lum: Norm-RGB-lum method produces the gray-level image by perform Luminance normalization after Norm-RGB normalization [Umbaugh, Solt, 2008].

Figures 4.3a through 4.3e show an original image and four corresponding color normalization images.

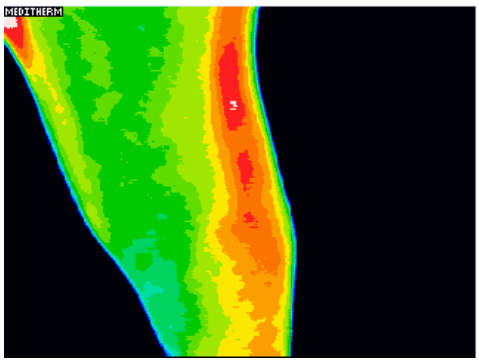

Figure 5a – Original Image

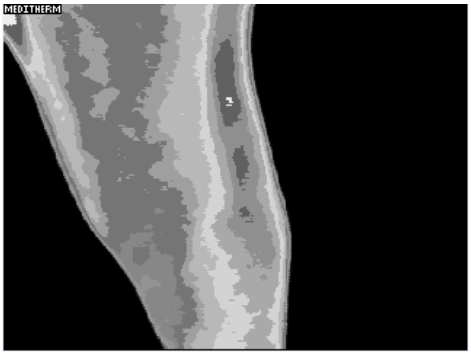

Figure 5b – Luminance Image

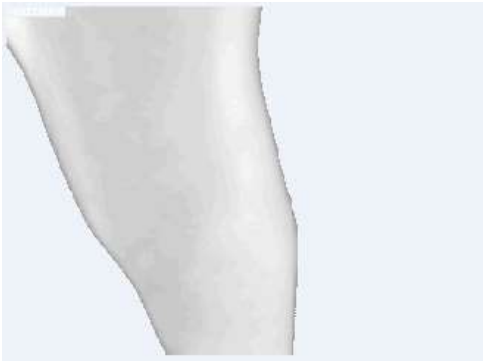

Figure 5c – NormRGB Image

Figure 5d – NormGrey Image

Figure 5e – NormRGB-lum Image

Figure 4.3 An Original Image and Four Corresponding Color Normalization Images

4.3 Feature Extraction

Feature extraction is important to simplify the raw image data into higher level, meaningful information. After color normalization of the original image, the feature extraction operation is performed. To eliminate redundancy in a huge amount of data, such as an image the input data will be transformed into a reduced representation as a feature vector. That is to transform the input image into a set of features. After that, feature analysis involves examining the features extracted from the images and determining how they can be used to solve the imaging problem under consideration [Umbaugh;2011]

Feature extraction starts with feature selection. "The selected features will be the major factor that determines the complexity and success of the analysis and pattern classification process [Umbaugh;2011]". In this research, histogram features, spectral features, texture features are used. Either original images or color normalized images can be used to extract these features by using CVIP-FEPC. While using the original image, four types of histogram features including histogram standard deviation, skew, energy, and entropy, five types of texture features include texture energy, inertia, correlation, inverse difference, and entropy with a texture distance(pixel) of 6, spectral feature with three rings and three sectors measurement are utilized. The histogram mean feature is the additional feature while using color normalized images for feature extraction because the histogram mean feature reflect the average temperature data.

Gabor filters are bandpass filters which are used for feature extraction and feature analysis. A set of Gabor filters with different frequencies and orientations are helpful for feature extraction from images. A comparison between original feature vectors and the Gabor feature vectors has been discussed in this study.

4.3.1 Histogram features

Histogram provides account of pixels versus the gray-level distribution for the image or sub-image. The histogram of an image is the frequency gray-level distribution with number of pixels for each value [Umbaugh;2011]. Four types of histogram features for the original images or five types of features for the color normalized images are selected with three bands of red, green, blue (RGB) in this research include histogram mean, standard deviation, skew, energy, and entropy.

The mean is the average value which represents the brightness of the image.

$$Mean = \sum_{r}\sum_{c}\frac{I(r,c)}{M}$$

where M is the number of pixel in image or subimage.

A bright image will have a high mean value whereas dark image will have a low mean value.

The standard deviation which is known as the square root of the variance describes the contrast of image.

$$\sigma_g = \sqrt{\sum_{g=0}^{L-1}(g-\bar{g})^2 P(g)} \quad \text{and } P(g) = \frac{N(g)}{M}$$

The skew measures the asymmetry about the mean in the gray-level distribution.

$$Skewness = \frac{1}{\sigma_g^3}\sum_{g=0}^{L-1}(g-\bar{g})^3 P(g) \text{ and } P(g) = \frac{N(g)}{M}$$

The skew will be positive if the tail of the histogram spreads to the right, and negative if the tail of the histogram spreads to the left.

The energy measure shows how the gray levels are distributed.

$$Energy = \sum_{g=0}^{L-1} [P(g)]^2 \ \ and \ \ P(g) = \frac{N(g)}{M}$$

The entropy is a measure for counting how many bits need to code the image data.

$$Entropy = -\sum_{g=0}^{L-1} P(g) \log_2 [P(g)] \ and \ \ P(g) = \frac{N(g)}{M}$$

A complex image has higher entropy than a simple image. Entropy measure tends to vary inversely with the energy measure [Umbaugh; 2011].

4.3.2 Spectral features

Spectral features, or frequency/sequency-domain based features are special features and the primary metric is power. The power spectrum is calculated by the magnitude of the spectral components squared:

Power = $|T\ (u, v)|^2$

The generic T(u,v) could be used in any transforms which typically use the Fourier transform. The spectral features are measured by calculating the power in various spectral regions, and these regions could be rings, sectors, or boxes. The sector measurement could find power of specific orientation regardless the frequency, while the ring measurement

could find the power of specific orientation whatever the orientation. In this study, three rings and three sectors are used.

4.3.3 Texture features

Texture is a visual pattern attribute. It is a property of areas, and consisting of sub-patterns which are related to the pixel distribution in a region [André; 2010].Texture features reflect properties including: smoothness, coarseness, roughness and regular patterns.

One method for measuring texture feature is to use the second-order histogram of the gray levels. Texture features involved with second order histograms are used for purposes of texture classification or segmentation. The second order histogram methods are also referred to as gray-level co-occurrence matrix or gray-level dependency matrix methods which use a second order histogram could count based on pairs of pixels and corresponding gray levels. These are two parameters important for these features: distance and angle. Distance is the distance between the pairs of pixels which are utilized by the second order statistics. The angle is the angle between the pairs of pixels. Usually, there are four different angles used: vertical, horizontal, left diagonal and right diagonal directions [Umbaugh; 2011].

Five types of texture features are used in this study including energy, inertia, correlation, inverse difference and entropy. The energy measures the smoothness by counting the distribution among the gray levels. The inertia shows the contrast while the correlation provides value of the similarities between pixels. The inverse difference measures the

homogeneity of the texture and entropy which inverse the energy being able to measure the information content [Umbaugh; 2011].

4.3.4 Gabor filter

The Gabor filter is a linear filter which is excellent for edge detection and has both frequency-selective and orientation-selective properties. Therefore the Gabor filter is particularly appropriate for texture discrimination, texture analysis and feature classification. Gabor feature vectors could be used as a classification or segmentation operator for new feature vector performance. In this study, the features extracted from Gabor filter were used for the new feature vectors that were used as input for the pattern classification.

The Gabor filter can be viewed as a sinusoidal wave of frequency and orientation, convolved by a Gaussian envelope. A 2-D Gabor filter acts as a local band-pass filter with specific frequency and orientation. Mathematically, in spatial domain, a 2D Gabor filter is the result of multiplication of a 2D Gaussian function and an exponential function, which can be represented as follow:

$$g(\lambda,\theta,\varphi,\sigma,\gamma) = \exp(-\frac{x(\theta)^2+\gamma^2 y(\theta)^2}{2\sigma^2})\exp(i(2\pi\frac{x(\theta)}{\lambda}+\varphi))$$

According Euler's formula $e^{i\theta} = \cos\theta + i.\sin\theta$, the complex form is expressed as a real number plus an imaginary number.Therefore, the complex Gabor filter could be separated with real and imaginary parts:

$$\text{Real: } g(\lambda,\theta,\varphi,\sigma,\gamma) = \exp(-\frac{x(\theta)^2+\gamma^2 y(\theta)^2}{2\sigma^2})\cos(2\pi\frac{x(\theta)}{\lambda}+\varphi)$$

$$\text{Imaginary: } g(\lambda,\theta,\varphi,\sigma,\gamma) = \exp(-\frac{x(\theta)^2+\gamma^2 y(\theta)^2}{2\sigma^2})\sin(2\pi\frac{x(\theta)}{\lambda}+\varphi)$$

Where $x(\theta)= x\cos\theta + y\sin\theta$, $y(\theta)= -x\sin\theta+y\cos\theta$

In this study, only the real part was considered.

For this equation, λ is wavelength of the sinusoidal factor. Therefore, $^1/_\lambda$ is the frequency of factor $\cos(2\pi\frac{x(\theta)}{\lambda}+\varphi)$. Figure 4.4 shows Gabor filter with four different wavelengths (λ) in spatial domain and Figure 4.5 shows Gabor filter with four different wavelengths (λ) in frequency domain.

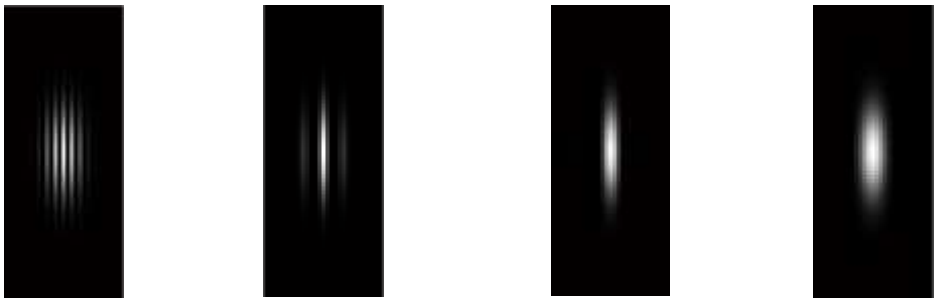

Figure 4.4 Four Different Wavelengths of Gabor Filter in Spatial Domain

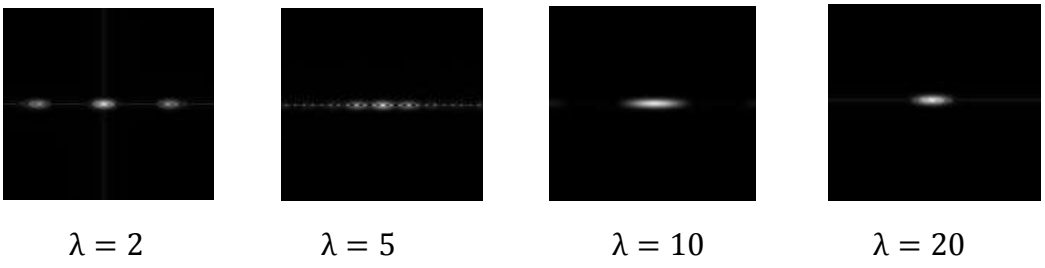

Figure 4.5 Four Different Wavelengths of Gabor Filter in Frequency Domain

θ is the orientation of the normal to the parallel stripes of a Gabor function. Figure 4.6 shows Gabor filter with three different orientations (θ) in spatial domain. 4.7 shows Gabor filter with three different orientations (θ) in frequency domain.

$\theta = 0$ $\theta = \pi/4$ $\theta = \pi/2$

Figure 4.6 Three Different Orientation of Gabor Filter in Spatial Domain

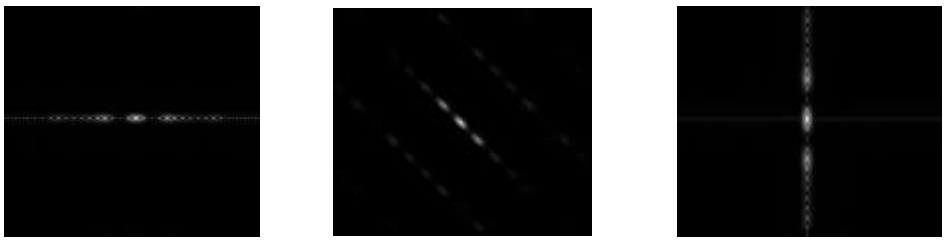

Figure 4.7 Three Different Orientation of Gabor Filter in Frequency Domain

φ is the offset of phase. σ represents the standard deviation of the Gaussian factor of the Gabor equation. γ is aspect ratio which reflect the ellipticity of Gabor equation which default value is 0.5.

Figure 4.8 shows Gabor filter with three different aspect ratios (γ).

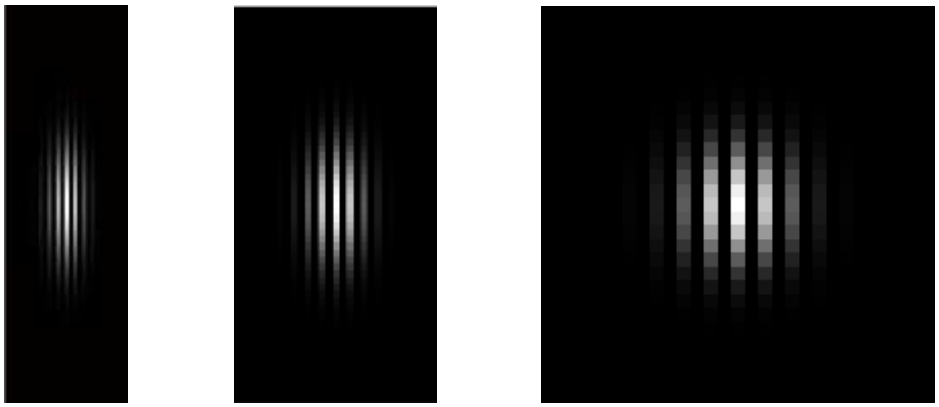

$\gamma = 0.3$ $\gamma = 0.5$ $\gamma = 1$

Figure 4.8 Three Different Aspect Ratios of Gabor Filter

b is the half-response spatial frequency bandwidth (in octaves) of a Gabor filter is related to the ratio σ / λ [Kruizinga ;1999]. .

$$b=\log_2 \frac{\frac{\sigma}{\lambda}\pi+\sqrt{\frac{\ln 2}{2}}}{\frac{\sigma}{\lambda}\pi-\sqrt{\frac{\ln 2}{2}}} \qquad \frac{\sigma}{\lambda}=\frac{1}{\pi}\sqrt{\frac{\ln 2}{2}}.\frac{2^b+1}{2^b-1}$$

Two two-dimensional Gabor filter with same standard deviation but different ratio provide different frequency and bandwidths. In Gabor function, the standard deviation of the Gaussian factor σ could be specified through bandwidth rather than specified directly. The default bandwidth is 1. Hence, $\sigma = 0.56\ \lambda$.

To investigate how Gabor filters perform for pattern classification via texture discrimination in thermographic images, code was implemented with Matlab. In Matlab, the Gabor filter was performed following by the real part formula which mentioned in this section. Four different equidistant orientations $[\theta = k * \left(\frac{\pi}{4}\right), k = 0,1,2,3]$ and three different

wavelength scales base on the texture of thermographic image are utilized. The rest of factors are used default value. Therefore, there are totally twelve different Gabor filters.

The next step is to convert the original thermographic images from color scale to grey scale to eliminate the error caused by the color shifting. The next step is convolving the grey scale images with different Gabor filters. The next step is to extract texture features from the Gabor filtered image to be used for pattern classification.

The Gabor filter function is related to the negative exponential form. And the kernel pixel values in the Gabor filter are very small values between -1 and 1.Thus, after being convolved with the grey image, the output image will have small values and may look like a black image. Therefore, the output image needs to be remapped back to [0,255]. Figure 4.9 shows grey image convolved with Gabor filter without remapping. Figure 4.10 shows grey image convolved with Gabor filter with remapping in spatial domain. Figure 4.11 shows grey image convolved with Gabor filter with remapping in frequency domain.

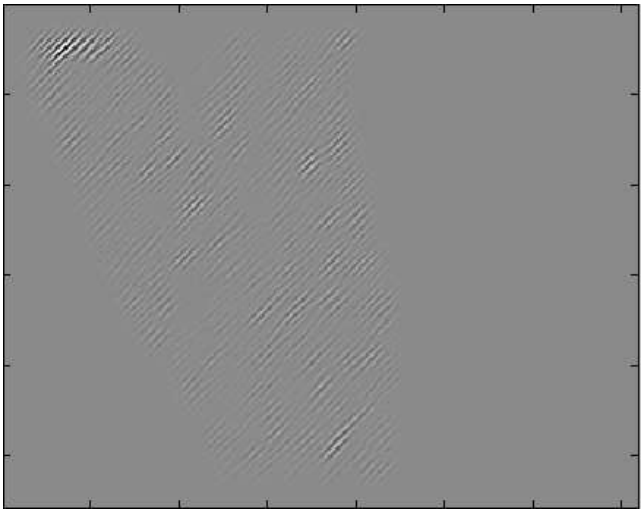

Figure 4.9 Grey Image Convolved With Gabor Filter without Remapping

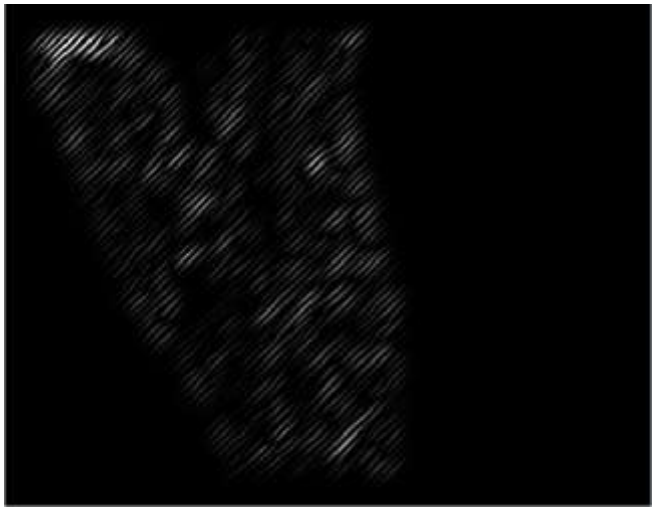

Figure 4.10 Grey Image Convolved Gabor Filter Remapping in Spatial Domain

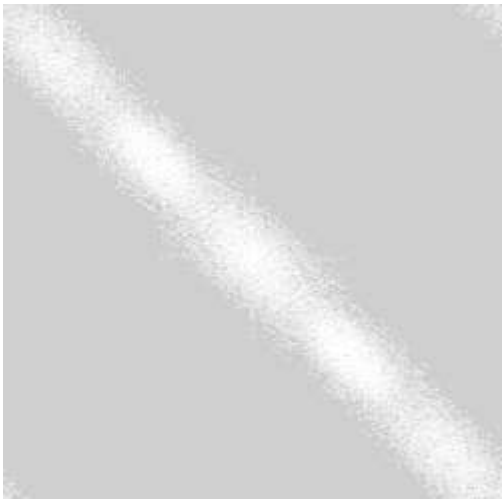

Figure 4.11 Grey Image Convolved Gabor Filter Remapping In Frequency Domain

The new output images are input to CVIP-FEPC to extract features followed by pattern classification in CVIP-FEPC.

4.4 Pattern Classification

Pattern classification uses the features to classify image objects which typically is the final step in the process. After different features have been extracted from raw images, feature analysis processing is necessary. Different features are selected by the variable selection methods which constitute feature vectors. The set of feature vectors need to be analyzed and prepared for developing the classification algorithm. The user needs to find the optimal combination of features which provide the best results. In the CVIP-FEPC, there are three steps for pattern classification including: data normalization, application of distance and/or similarity metrics, and the classification algorithm itself.

4.4.1 Data normalizaiton

Data normalization is adopted to avoid biasing distance and similarity measures due to the varying range on different vector components [Umbaugh; 2011]. There are several data normalization methods in CVIP-FEPC including: range-normalize, unit vector normalization, standard normal density normalization, min-max normalization, softmax scaling method. Standard normal density normalization and softmax scaling methods are used in this study. These two data normalization method provide better result comparing with others.

Standard normal density is a kind of statistical-based method which normalize the feature vector by subtracting the mean value and dividing by the standard deviation [Umbaugh; 2010] for each feature. The process is as follows:

$F_j = \{F_1, F_2, \ldots, F_k\}$, F_j is feature space which contain different k feature vectors. Every feature vector involves n features.

$$F_j = \begin{bmatrix} f_{1j} \\ f_{2j} \\ \vdots \\ f_{nj} \end{bmatrix} \quad \text{for } j = 1, 2, \ldots, k$$

Means: $m_i = \frac{1}{k} \sum_{j=1}^{k} f_{ij}$ for $i = 1, 2, \ldots, n$

Standard deviation: $\sigma_i = \sqrt{\frac{1}{k} \sum_{j=1}^{k} (f_{ij} - m_i)^2}$ for $i = 1, 2, \ldots, n$

Every feature component normalizes by subtracting the mean and then divides by the standard deviation.

$$f_{\text{ijSND}} = \frac{f_{ij} - m_i}{\sigma_i}$$

The new feature distribution on each vector after normalization is called standard normal density (SND).

Softmax scaling is a nonlinear method which is desired if the data distribution is skewed, that is not evenly distributed about the mean. Softmax will normalize the spread of data by moving the mean and rescaling the data range from 0 to 1 [Umbaugh; 2010]. There are two steps for softmax scaling method:

STEP1 $\Rightarrow y = \frac{f_{ij} - m_i}{r\sigma_i}$ where m_i is the mean value, f_{ij} is the feature vectors, σ_i is the standard deviation, r is the factor which is defined by the user.

Step 1 is similar with SND while r is the new factor which is defined by the user. The factor determines the range values of the feature f_{ij}.

STEP2 $\Rightarrow f_{\text{ijSMC}} = \frac{1}{1+e^{-y}}$ for all i, j

f_{ijSMC} is the feature after normalized. If y is small enough, this process is almost linear and the feature data is rescaled exponentially.

4.4.2 Distance and similarity measures

After feature extraction and normalization, comparison of two feature vectors is necessary to perform the pattern classification. The idea is basically to find the difference or similarity between two feature vectors. The difference can be measured by the distance measure in the feature space. The smaller distance between two feature vectors, the greater similarity and the less difference.

There are several distance measure and similarity measure method In CVIP-FEPC. In this study, the *Euclidean distance* measure has been utilized which frequently used for distance comparison in optimization problems.

Euclidean distance need to be measured by the square root of the sum of the squared of the differences between vector components [CVIPtools;2012].The process is showed as follow:

A and B are different feature vectors which both contain n feature components.

$$A = \begin{bmatrix} a_1 \\ a_2 \\ \vdots \\ a_n \end{bmatrix} \quad B = \begin{bmatrix} b_1 \\ b_2 \\ \vdots \\ b_n \end{bmatrix}$$

The Euclidean distance is:

$$D_E(A, B) = \sqrt{\sum_{i=1}^{n}(a_i - b_i)^2} = \sqrt{(a_1 - b_1)^2 + (a_2 - b_2)^2 + \cdots + (a_n - b_n)^2}$$

4.4.3 Classification algorithm

One method to develop a classification algorithm, requires that the feature data are separated into a training set and a test set. The training set consist of a set of training examples which is utilized for classification algorithm development and test set is used for testing the classification algorithm. To provide an unbiased result, both training set and test set should represent all types of classes in the application domain. Theoretically, maximizing size of the training set will provide the best while maximizing the size of the test set will provide maximum confidence that the test results will be a valid predictor for future results[Umbaugh;2011]. Leave-one-out cross validation method is used in this study which is a special case of training and test sets algorithm. With leave-one-out cross validation method, only one sample is left for the test set and rest of samples are marked as training set. This is done for each sample in the entire set.

In CVIP-FEPC, there are three classification algorithms available with leave-one-out method including: *Nearest Neighbor*, *K-Nearest Neighbor*, and *Nearest Centroid*. In this study, nearest neighbor and K-nearest neighbor methods were applied. For this research there are only fourteen images for the abnormal set, and the Nearest Centroid method is only appropriate with large data sets.

Nearest neighbor is the simplest classification algorithm which classifies the unknown as the closet sample in the training set by using distance measure or similarity measure. Therefore, it is not robust enough. K-nearest neighbor method could consider top k nearest neighbors to the query. K=5 was used in this research. For the previous experiments, K=5 could perform better result comparing with 3 and 7. [Umbaugh;2011]

4.4.4 Success measure and evaluation

The success rate measures classification accuracy. Sensitivity and Specificity are two statistical measures of success evaluation , often used in medical studies, which have the following definitions:

- True Positive (TP): sick person classified correctly.
- False Positive (FP): healthy person classified as sick.
- True Negative (TN): healthy person classified correctly.
- False Negative (FN): sick person classified as healthy.

The relationship with True Positive (TP), False Positive (FP), True Negative (TN), False Negative (FN) could be showed as:

	Condition positive	Condition negative
Test positive	True Positive (TP)	False Positive (FP)
Test negative	False Negative (FN)	True Negative (TN)

Sensitivity and Specificity are defined as follow:

$$\text{Sensitivity} = \frac{number\ of\ True\ Positives}{number\ of\ True\ positives + number\ of\ False\ Positives}$$

$$\text{Specificity} = \frac{number\ of\ True\ Negatives}{number\ of\ True\ Negatives + number\ of\ False\ Positives}$$

Sensitivity indicates how accurate of identifying a disease as prediction and Specificity indicates how accurate prediction of absence of the disease is [Umbaugh;2011].

CHAPTER 5

RESULTS AND ANALYSIS

The goal of the research is to determine the accurate of thermographic image analysis in detection of canine ACL disease. The result of the research is separated into two sections. In the first section, the result is obtained by using the features extracted from CVIP-FEPC which involve histogram features, texture features and spectral feature for pattern classification. In the second section, the result is utilizing the new feature vector from images which were convolved by the Gabor filter for pattern classification.

5.1 ACL Disease Detection by Using CVIP-FEPC

Based on different views of the canines, the 168 images from 28 canines have been divided into three groups: 1) anterior view, 2) lateral view, 3) posterior view. Every group includes 56 images with 14 abnormal images and 42 normal images. The images are categorized into two classes: *Normal* and *Abnormal*. All three groups of images are processed with performed color normalization operations. Different features extraction and pattern classification methods are performed in CVIP-FPEC.

5.1.1 Anterior view

In this section, the result of the anterior view is discussed and analyzed. The thermographic images are taken from in front of the canine for this view. As mentioned in the Chapter 4, there are totally five different experiments including one experiment using original images and four experiments using the color-normalized images. The original images use ten different features with four histogram features, five texture features and

spectral features. To perform all the combinations of the feature vectors, totally $2^{10} - 1$=1023 combined feature sets have been formed. Color normalized images which contain the additional feature of the histogram mean, for a total of eleven features with five histogram features, five texture features and spectral feature. Hence there are total of $2^{11} - 1$=2047 combined feature sets for the color normalized images. These feature vectors extracted with CVIP-FPEC are data normalized with standard normal density normalization method and softmax scaling normalization method. In this study, the Euclidean distance measure is used as the distance measure. Nearest neighbor and K-nearest neighbor where K=5 are utilized as classification methods in these experiments and leave one out is used as the testing method.

The best result for original and four different color normalization experiments of anterior view are shown in Table 5.1.

Table 5.1 Results for Original and Color Normalized Images of Anterior View Group

Color Normalization Method	Camera View	Classification Success Rate
Original	Anterior	78.57%
Lum	Anterior	78.57%
NormGrey	Anterior	83.93%*
NormRGB	Anterior	78.57%
NormRGB-Lum	Anterior	82.14%

The classification success rate is the numbers of objects correctly matching the predicted categories for normal or abnormal class. As the result shown in Table 5.1, the classification success rate of images which involved the color normalization methods always obtain the same or better result than the original images. Among these methods, the best classification success rate is from NormGrey images with 83.93%.

More details of features combinations and classification method for anterior group are shown in Table 5.2.

Table 5.2 Results for Original and Color Normalized Images of Anterior View Group

Color Normalization Method	Features	Normalization Method	Classification Methods	Classification Success
Original	Spectral Texture Inertia Texture Entropy	Soft-max, r = l	KNN=5	78.57%. Sensitivity:14.29% Specificity:100.00%
Lum	Texture InvDiff Histogram Mean	Soft-max, r = l	NN	78.57%. Sensitivity:42.86% Specificity: 90.48%
NormGrey	Texture Inertia Histogram StdDev	None	NN	83.93%.* Sensitivity: 71.43% Specificity: 88.10%
NormRGB	Texture InvDiff Histogram StdDev Histogram Energy	Soft-max, r = l	KNN=5	78.57%. Sensitivity:21.43% Specificity:97.62%
NormRGB-Lum	Histogram StdDev Histogram Energy	Soft-max, r = l	NN	82.14%. Sensitivity:64.29% Specificity:88.10%

In accordance with Table 5.2, the best result of anterior view is from NormGrey color normalized method. The combination of texture inertia feature and histogram standard deviation feature provides the highest success rate. From the results of five experiments, histogram standard deviation is the most frequently used feature and Soft-max is the best method for data normalization. The result from the original images shows great specificity (100.00%) but very low sensitivity (14.29%). Both four color normalized methods did improve the sensitivity. The NormGrey image sets increase 57.14% which is a significant improvement.

5.1.2 Lateral view

In this section, the result of the anterior view is discussed and analyzed. The same 28 dogs but different image views are utilized. Lateral view experiments are performed using the same classification methods and testing methods tgat were used with the anterior view images. They are also implemented by using CVIP-FPEC with identical features of previous experiments. The best results of lateral view group experiments are shown in Table 5.3. In the lateral group view experiments, NormGrey and NormRGB provide best success rates with 83.93% each. The best combination of features sets for original and four different color normalized methods are shown in Table 5.4

Table 5.3 Results for Original and Color Normalized Images of Lateral View Group

Color Normalization Method	Camera View	Classification Success Rate
Original	Lateral	78.57%
Lum	Lateral	78.57%
NormGrey	Lateral	83.93%*
NormRGB	Lateral	83.93%*
NormRGB-Lum	Lateral	82.14%

Table 5.4 Detail for Original and Color Normalized Images of Lateral View Group

Color Normalization Method	Features	Normalization Method	Classification Methods	Classification Success
Original	Spectral Texture InvDiff Histogram StdDev Histogram Entropy	Soft-max, r = l	NN	78.57%. Sensitivity:42.86% Specificity:90.48%
Lum	Texture Correlation Histogram Skew	None	KNN=5	78.57% Sensitivity:28.57% Specificity:95.24%
NormGrey	Texture Energy Texture Inertia Texture Correlation Texture InvDiff Histogram Mean Histogram Energy	Soft-max, r = l	NN	83.93%* Sensitivity:57.14% Specificity:92.86%
NormRGB	Texture InvDiff	Soft-max, r = l	KNN=5	83.93%* Sensitivity:57.14% Specificity:92.86%
NormRGB-Lum	Texture InvDiff Histogram StdDev Histogram Entropy	Soft-max, r = l	NN	82.14% Sensitivity:71.43% Specificity:85.71%

According to Table 5.4, the most frequent feature used for the lateral view experiments is Texture Inverse Difference feature. Soft-max is also the best method for data normalization.

5.1.3 Posterior view

In this section, the result of posterior view is discussed and analyzed. The thermographic images for this view are taken behind looking toward the front of the canine. A total of 56 images with 42 normal images and 14 abnormal images are applied. The experimental method of this view is kept the same with anterior and lateral view. Table 5.5 shows the overall result of original and four different color normalized sets of image.

Original images and NormRGB-lum images provide the best success rate with 82.14%. Table 5.6 displays the best combination of features sets for original and four different color normalized methods.

Table 5.5 Results for Original and Color Normalized Images of Posterior View Group

Color Normalization Method	Camera View	Classification Success Rate
Original	Posterior	80.35%
Lum	Posterior	80.35%
NormGrey	Posterior	80.35%
NormRGB	Posterior	80.35%
NormRGB-Lum	Posterior	82.14%*

Table 5.6 Detail for Original and Color Normalized Images of Posterior View Group

Color Normalization Method	Features	Normalization Method	Classification Methods	Classification Success
Original	Texture Energy Texture InvDiff Texture Entropy Histogram StdDev Histogram Skew	Soft-max, r = l	KNN=5	80.35% Sensitivity:28.57% Specificity:97.62%
Lum	Texture Entropy Histogram Mean Histogram StdDev	Soft-max, r = l	KNN=5	80.35% Sensitivity:28.57% Specificity:97.62%
NormGrey	Texture Inertia Histogram Skew Histogram Energy	Soft-max, r = l	KNN=5	80.35% Sensitivity:42.86% Specificity:92.86%
NormRGB	Texture Correlation Texture Entropy Histogram Energy	Standard Normal Density	KNN=5	80.35% Sensitivity:42.86% Specificity:92.86%

NormRGB-Lum	Texture Correlation Histogram Mean Histogram StdDev Histogram Skew Histogram Entropy	Standard Normal Density	NN	82.14%. Sensitivity:57.14% Specificity:92.86%

5.1.4 Summary

The objective of this project is to investigate the efficacy of feature extraction and pattern classification with thermographic images for the canine ACL project. There are a total of fifteen sets of experiments performed in this section: three views of images with five different color normalization methods. In order to evaluate the best classification success rate among these fifteen groups of experiments more explicitly, the result are reflect into graph type. Figure 5.1 displays the best results from anterior view, lateral view and posterior view obtained from CVIP-FEPC.

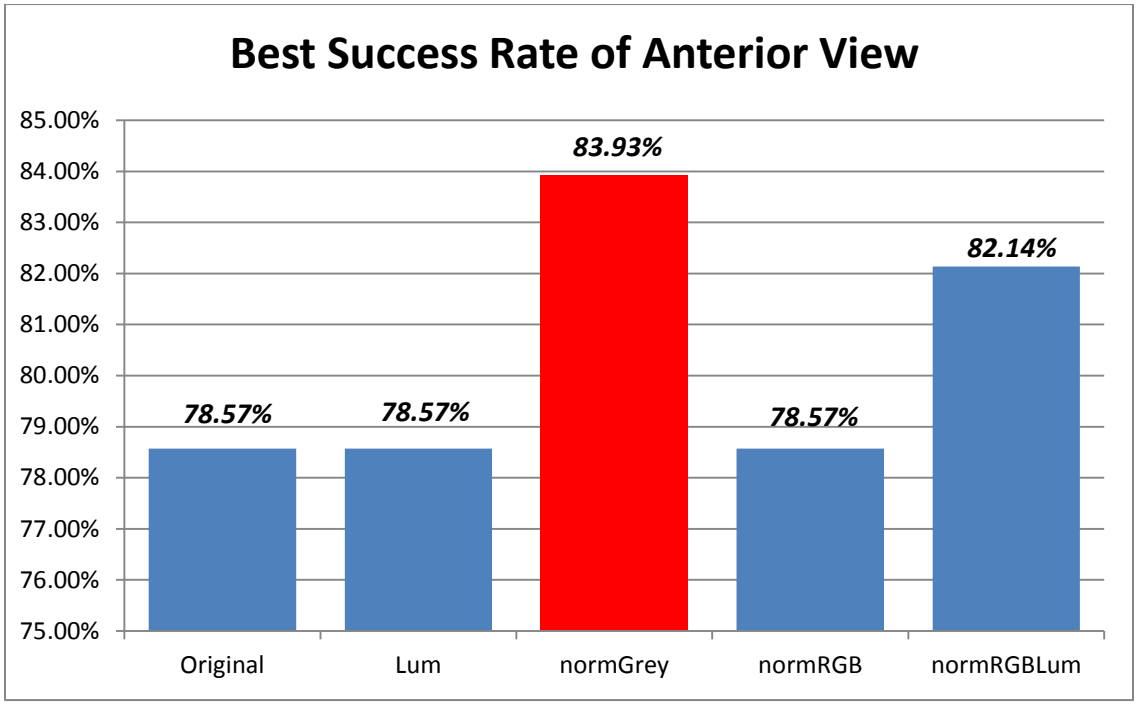

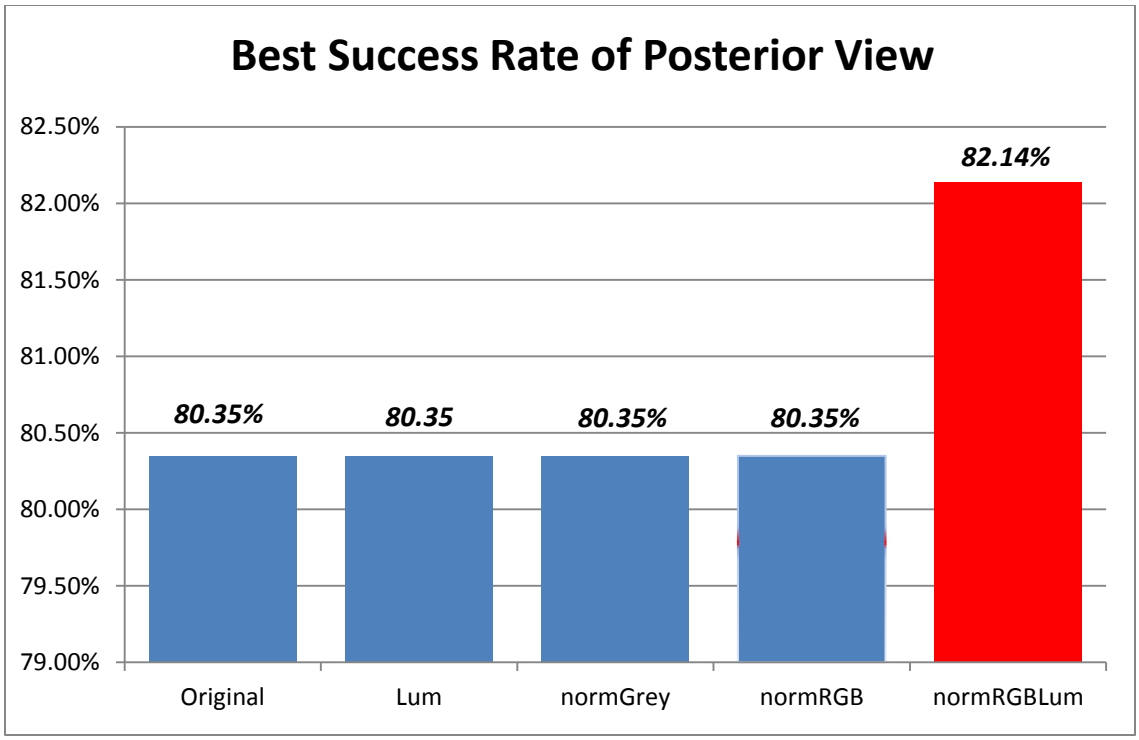

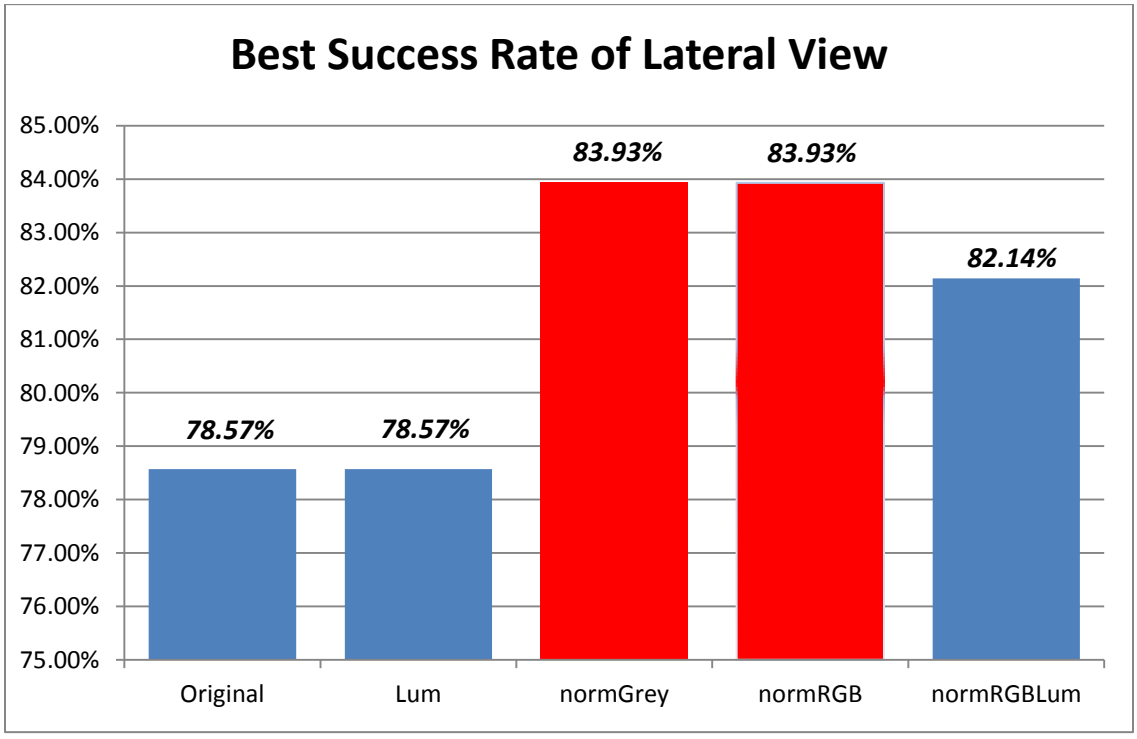

Figure 5.1 The Best Success Result with Different Color Normalization Methods

As shown in Figure 5.1, the best classification success rate among these fifteen groups is 83.93%.This value is achieved by anterior view images with NormGrey color normalization with 71.43% Sensitivity, 88.10% Specificity and lateral view images with NormGrey and NormRGB color normalization with 57.14% Sensitivity and 92.86% Specificity. Therefore, NormGrey is the best color normalization. To investigate which features is more useful for classification. Figure 5.2 shows the frequency of different eleven features being used in these fifteen groups of experiments.

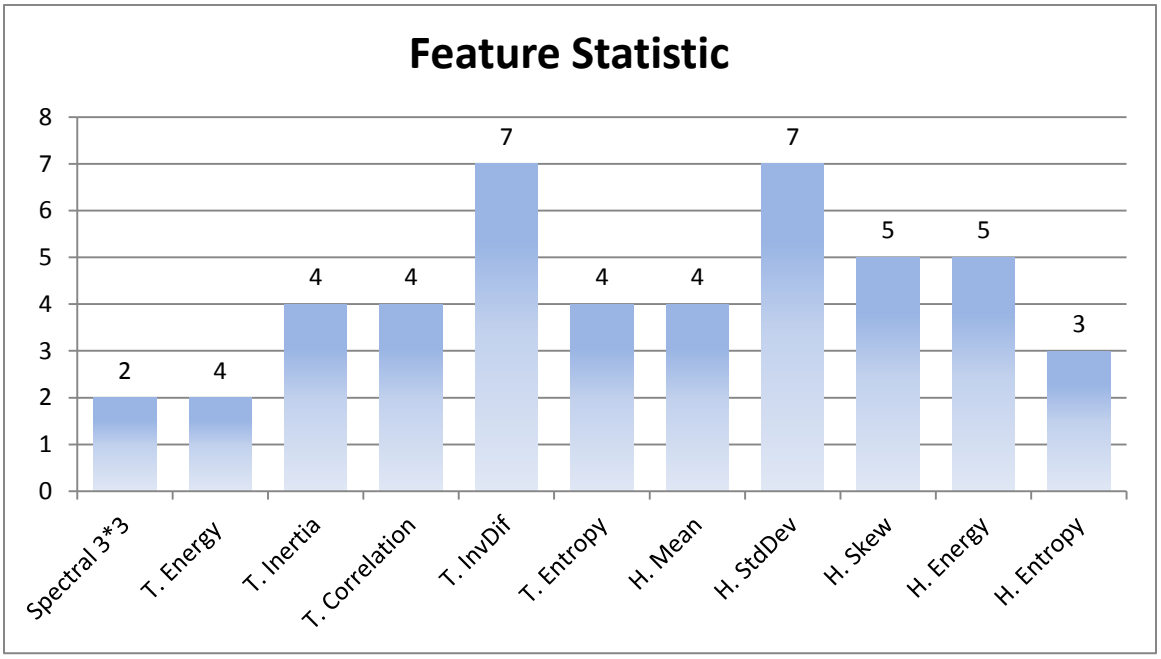

Figure 5.2 The Statistic of Features with Best Result of Fifteen Experiments.

According to Figure 5.2, Texture Inverse Different feature and Histogram Standard Deviation feature are the most frequent features used in these fifteen experiments.

5.2 Using Gabor Filter in Thermographic Image for ACL Detection

In this section, Gabor filter i used for new feature vector extraction. As mention in chapter 4.3.4, a 2-D Gabor filter acts as a local band-pass filter with a specific frequency and orientation. Mathematically, a 2D Gabor function is the product of a 2D Gaussian and a complex exponential function, which can be represented as follow:

$$\text{Real: } g(\lambda, \theta, \varphi, \sigma, \gamma) = \exp\left(-\frac{x(\theta)^2+\gamma^2 y(\theta)^2}{2\sigma^2}\right)\cos\left(2\pi\frac{x(\theta)}{\lambda}+\varphi\right)$$

The code for Gabor filter is implemented in Matlab. To investigate how effective the Gabor filters features are for the ACL classification with thermographic images, four

different equidistant orientations $[\theta = k * \left(\frac{\pi}{4}\right), k = 0,1,2,3]$ and three different wavelength scales $(\lambda = 3.5,4.0,4.5)$ based on the thermographic images are utilized. Consequently, twelve different Gabor filters are performed. The offset of phase φ uses a default value zero which means no phase shifting for the cosine factor. Aspect ratio γ which represents the ellipticity keeps at a constant value of 0.5. The standard deviation σ is defined as 2.8.

The same 168 images with three different views as used in previously described experiments are used in this section. To avoid color shifting, the original images have been directly converted to grey level images by using CVIPtools. Then the grey level images are convolved with twelve different Gabor filters separately. Because of the negative exponential form, the range of pixel value of output images is between -1 and 1. To transfer back to the original data range [0,255], a remapping process has been performed to the output in Matlab. Finally, the remapped outputs are used for new feature vector extraction and pattern classification.

5.2.1 Anterior view

There are a total of 56 images used in this group 42 normal images and 14 abnormal images. The features are selected identically as in section 5.1.1. Eleven different features with five histogram features, five texture features and spectral feature are used. Hence there are in total of $2^{11} - 1$=2047 combined feature sets. These Gabor feature vectors extracted from CVIP-FPEC are data normalized with standard normal density normalization and softmax scaling normalization methods. In this study, the Euclidean distance measure is used as the distance measure. These experiments use nearest neighbor and K-nearest neighbor where K=5 as classification methods and leave one out as the testing method. Table 5.7 shows the anterior view result of wavelength $(\lambda) = 3.5$, 4.0 and 4.5.

Table 5.7a Results Involved Gabor Filter with 3.5 Wavelength of Anterior View Group

Orientation	Number of Images per Class	Camera View	Normalization Method	Classification Methods	Classification Success Rate
0	Normal: 42 Abnormal: 14	Anterior	Standard Normal Density	KNN=5	83.92% Sensitivity:71.43% Specificity:88.10%
$\pi/4$	Normal: 42 Abnormal: 14	Anterior	Standard Normal Density	KNN=5	87.50%* Sensitivity:71.43% Specificity:92.86%
$\pi/2$	Normal: 42 Abnormal: 14	Anterior	Soft-max, r = l	NN	83.92% Sensitivity:71.43% Specificity:88.10%
$3\pi/4$	Normal: 42 Abnormal: 14	Anterior	Standard Normal Density	KNN=5	80.36% Sensitivity:50.00% Specificity:90.48%

Table 5.7b Results Involved Gabor Filter with 4 Wavelength of Anterior View Group

Orientation	Number of Images per Class	Camera View	Normalization Method	Classification Methods	Classification Success Rate
0	Normal: 42 Abnormal: 14	Anterior	Soft-max, r = l	KNN=5	82.14% Sensitivity:64.29% Specificity:88.10%
$\pi/4$	Normal: 42 Abnormal: 14	Anterior	Standard Normal Density	NN	83.92% Sensitivity:71.43% Specificity:88.10%

$\pi/2$	Normal: 42 Abnormal: 14	Anterior	Soft-max, r = l	KNN=5	83.92% Sensitivity:71.43% Specificity:88.10%
$3\pi/4$	Normal: 42 Abnormal: 14	Anterior	Standard Normal Density	NN	82.14% Sensitivity:57.14% Specificity:90.48%

Table 5.7c Results Involved Gabor Filter with 4 Wavelength of Anterior View Group

Orientation	Number of Images per Class	Camera View	Normalization Method	Classification Methods	Classification Success Rate
0	Normal: 42 Abnormal: 14	Anterior	Standard Normal Density	KNN=5	82.14% Sensitivity:64.29% Specificity:88.10%
$\pi/4$	Normal: 42 Abnormal: 14	Anterior	Standard Normal Density	KNN=5	82.14% Sensitivity:64.29% Specificity:88.10%
$\pi/2$	Normal: 42 Abnormal: 14	Anterior	Soft-max, r = l	KNN=5	80.36% Sensitivity:50.00% Specificity:90.48%
$3\pi/4$	Normal: 42 Abnormal: 14	Anterior	Standard Normal Density	KNN=5	80.36% Sensitivity:64.29% Specificity:90.48%

According to the Table 5.7, the parameter of best result of anterior group is wavelength $(\lambda) = 3.5$ with 45 degree, which provide 87.50% success rate.

5.2.2 Lateral view

In this section, the results of lateral view images using the Gabor filter features are discussed. The 56 the images from lateral view are taken from same dogs. The data normalized methods and classification methods are kept the same in anterior group. In

addition, the parameter in the Gabor filter is also performed with four orientations and three wavelengths. Those results are displayed in Table 5.8.

Table 5.8a Results Involved Gabor Filter with 3.5 Wavelength of Lateral View Group

Orientation	Number of Images per Class	Camera View	Normalization Method	Classification Methods	Classification Success Rate
0	Normal: 42 Abnormal: 14	Lateral	Standard Normal Density	KNN=5	82.14% Sensitivity:64.28% Specificity:88.10%
$\pi/4$	Normal: 42 Abnormal: 14	Lateral	Standard Normal Density	KNN=5	83.92%* Sensitivity:71.43% Specificity:88.10%
$\pi/2$	Normal: 42 Abnormal: 14	Lateral	Soft-max, r = l	KNN=5	83.92%* Sensitivity:71.43% Specificity:88.10%
$3\pi/4$	Normal: 42 Abnormal: 14	Lateral	Standard Normal Density	KNN=5	80.36% Sensitivity:50.00% Specificity:90.48%

Table 5.8b Results Involved Gabor Filter with 4 Wavelength of Lateral View Group

Orientation	Number of Images per Class	Camera View	Normalization Method	Classification Methods	Classification Success Rate
0	Normal: 42 Abnormal: 14	Lateral	Soft-max, r = l	KNN=5	82.14% Sensitivity:64.29% Specificity:88.10%
$\pi/4$	Normal: 42 Abnormal: 14	Lateral	Standard Normal Density	KNN=5	83.92%* Sensitivity:71.43% Specificity:88.10%
$\pi/2$	Normal: 42 Abnormal: 14	Lateral	Soft-max, r = l	KNN=5	82.14% Sensitivity:64.28% Specificity:88.10%
$3\pi/4$	Normal: 42 Abnormal: 14	Lateral	Standard Normal Density	NN	78.57% Sensitivity:50.00% Specificity:88.10%

Table 5.8c Results Involved Gabor Filter with 4.5 Wavelength of Lateral View Group

Orientation	Number of Images per Class	Camera View	Normalization Method	Classification Methods	Classification Success Rate
0	Normal: 42 Abnormal: 14	Lateral	Standard Normal Density	NN	80.36% Sensitivity:64.29% Specificity:88.10%
$\pi/4$	Normal: 42 Abnormal: 14	Lateral	Standard Normal Density	KNN=5	82.14% Sensitivity:64.29% Specificity:88.10%
$\pi/2$	Normal: 42 Abnormal: 14	Lateral	Standard Normal Density	KNN=5	82.14% Sensitivity:50.00% Specificity:90.48%
$3\pi/4$	Normal: 42 Abnormal: 14	Lateral	Standard Normal Density	KNN=5	80.36% Sensitivity:64.29% Specificity:90.48%

From the Table 5.8, there are three experiments provide the best success rate with 83.92%.Two of them are from $\lambda = 3.5$ group with 45 and 90 degrees. Another one is from the $\lambda = 4.0$ group with 45 degrees.

5.2.3 Posterior view

In this section, the results of posterior view images involved Gabor filter are discussed. The 168 of the images from posterior view are taken from same dogs. The data normalized methods and classification methods are kept the same in anterior group. In addition, the parameter in the Gabor filter is also performed with four orientations and three wavelengths. The results are displayed in Table 5.9.

Table 5.9a Results Involved Gabor Filter with 3.5 Wavelength of Posterior View Group

Orientation	Number of Images per Class	Camera View	Normalization Method	Classification Methods	Classification Success Rate
0	Normal: 42 Abnormal: 14	Posterior	Soft-max, r = l	KNN=5	80.36% Sensitivity:71.43% Specificity:88.10%
$\pi/4$	Normal: 42 Abnormal: 14	Posterior	Standard Normal Density	KNN=5	85.71%* Sensitivity:71.43% Specificity:90.48%
$\pi/2$	Normal: 42 Abnormal: 14	Posterior	Soft-max, r = l	NN	82.14% Sensitivity:64.29% Specificity:88.10%
$3\pi/4$	Normal: 42 Abnormal: 14	Posterior	Standard Normal Density	KNN=5	82.14% Sensitivity:64.29% Specificity:88.10%

Table 5.9b Results Involved Gabor Filter with 4 Wavelength of Posterior View Group

Orientation	Number of Images per Class	Camera View	Normalization Method	Classification Methods	Classification Success Rate
0	Normal: 42 Abnormal: 14	Posterior	Soft-max, r = l	KNN=5	82.14% Sensitivity:64.29% Specificity:88.10%
$\pi/4$	Normal: 42 Abnormal: 14	Posterior	Standard Normal Density	NN	85.71%* Sensitivity:71.43% Specificity:90.48%
$\pi/2$	Normal: 42 Abnormal: 14	Posterior	Standard Normal Density	KNN=5	85.71%* Sensitivity:71.43% Specificity:90.48%
$3\pi/4$	Normal: 42 Abnormal: 14	Posterior	Standard Normal Density	KNN=5	82.14% Sensitivity:57.14% Specificity:90.48%

Table 5.9c Results Involved Gabor Filter with 4.5 Wavelength of Posterior View Group

Orientation	Number of Images per Class	Camera View	Normalization Method	Classification Methods	Classification Success Rate
0	Normal: 42 Abnormal: 14	Posterior	Standard Normal Density	KNN=5	82.14% Sensitivity:64.29% Specificity:88.10%
$\pi/4$	Normal: 42 Abnormal: 14	Posterior	Standard Normal Density	KNN=5	83.92% Sensitivity:71.43% Specificity:88.10%
$\pi/2$	Normal: 42 Abnormal: 14	Posterior	Soft-max, r = l	KNN=5	85.71%* Sensitivity:71.43% Specificity:90.48%
$3\pi/4$	Normal: 42 Abnormal: 14	Posterior	Soft-max, r = l	KNN=5	82.14% Sensitivity:64.29% Specificity:88.10%

5.2.4 Summary

To determine how Gabor feature vectors are helpful for detecting ACL disease, a total of 36 experiments are performed with CVIP-FEPC. The results obtained with the Gabor features are remarkable. In this study, the Gabor filters are implemented with four different preferred orientations and three preferred spatial-frequencies. The results of each of the three sets of experiments (Table 5.7 through 5.9) are shown in Figure 5.3, in which the best classification success rate 87.50%. $\pi/4$ and $\pi/2$ are the optimal orientations which provide best result in different sets.

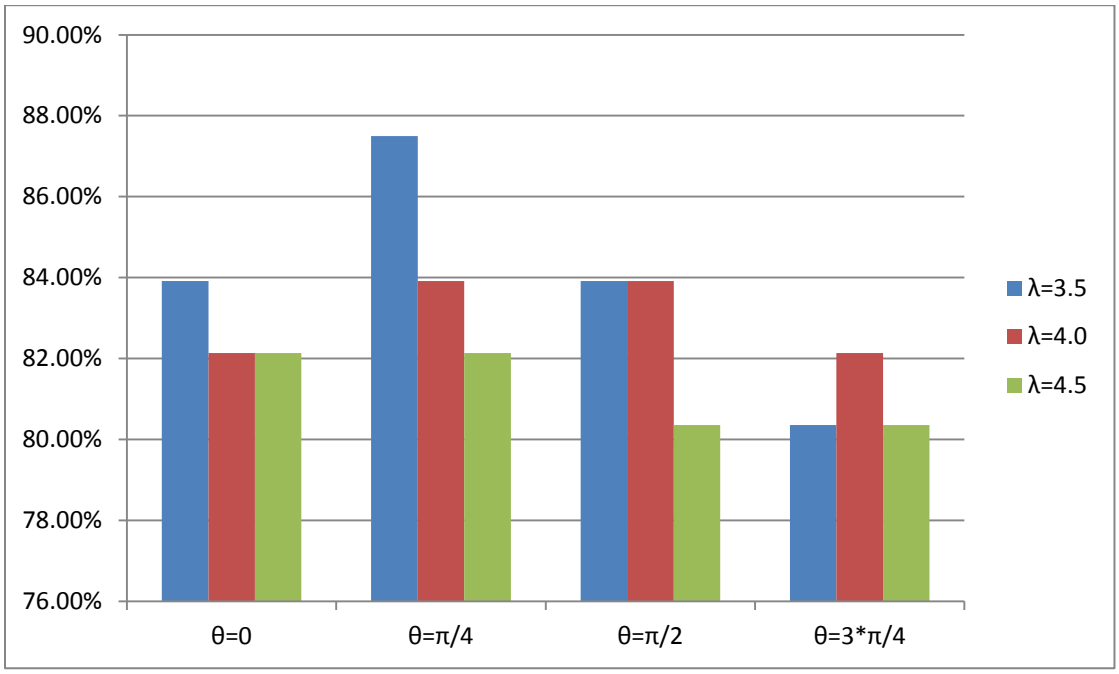

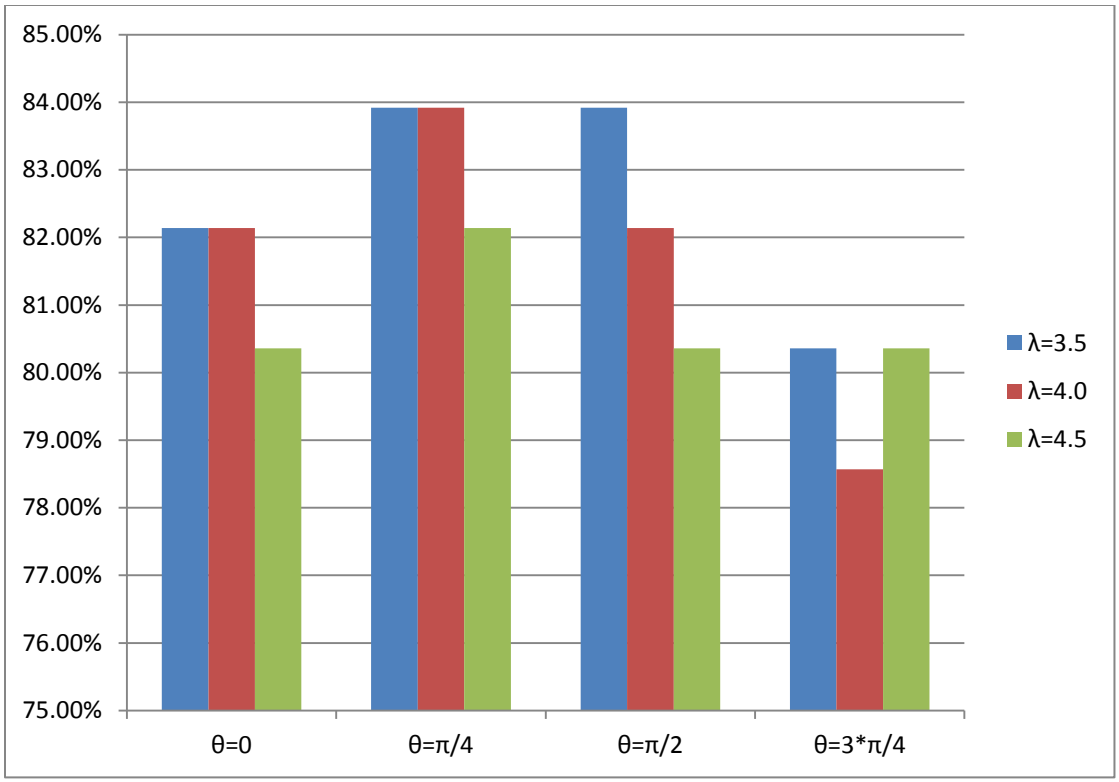

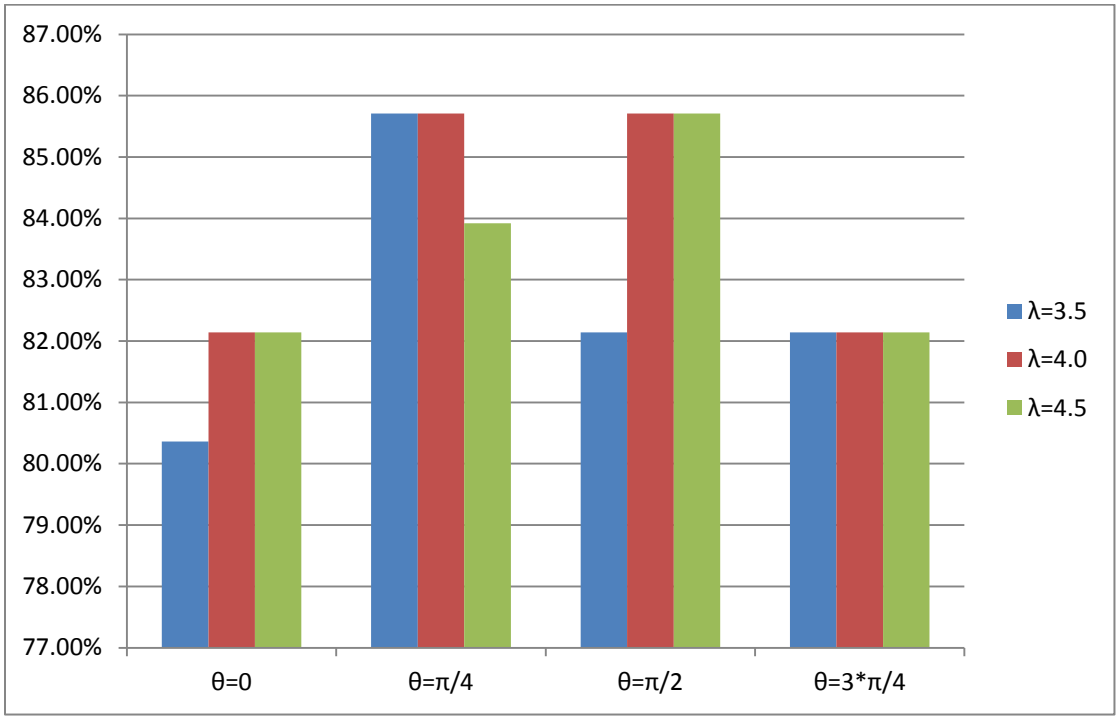

Figure 5.3 Best Success Rate by Involving Gabor Filter with Different Parameters

CHAPTER 6

SUMMARY AND CONCLUSION

Canine anterior cruciate ligament (ACL) rupture is a common disease problem in canines. The MRI (Magnetic resonance imaging) is the standard method to diagnosis this disease. However, MRI is expensive and time-consuming, and difficult to use with animals. Therefore, it is necessary to find an alternative diagnostic method. In this research, thermographic images are utilized as a prescreening tool for detection of ACL ruptures. A quantitative comparison is made of new feature vectors which are based on the Gabor filter with different frequencies and orientations. The best success rate of first/second-order histogram and specture features is 83.93% for ACL rupture disease detection. Additionally, the new features vectors using Gabor filter improve the result to 87.50% with 71.43% sensitivity and 92.86% specificity.

Thermographic images of 28 dogs with 14 normal and 14 abnormal were obtained from the Long Island Veterinary Specialists (LIVS). All dogs in the normal group have no orthopedic issues currently or in the past. Of the dogs in the abnormal group, only one leg is affected by ACL rupture disease and the opposite leg is considered normal. There are total of 168 images involved in this study. They have been separated into three groups based on the view of camera: anterior, lateral, posterior view. Each group has 56 images.

Fifteen sets of experiments with original and four types of color normalized images are performed using the two classes *normal* and *abnormal*. The best classification rate for the anterior view is 83.93% which is produced by the NormGrey images. The best classification rate of lateral view is 83.93% which is from NormGrey and NormRGB images. The best

classification rate of the lateral view is 82.14% which is from NormRGB-lum images. Upon three group experiments, the best result is always provided by color normalized images. Therefore, color normalization does improve the experimental result. Comparing the average success rate of three groups, the lateral view images are the best.

The Gabor filter has both frequency-selective and orientation-selective properties which is excellent for texture discrimination and segmentation. To determine how the Gabor filter is helpful for using thermographic images to detect ACL disease, a total of 36 experiments with the Gabor filter based features with involved four orientations and three scales of frequency were performed. With anterior, lateral and posterior view images, the best classification success rate 87.50%, 83.93%, 85.71% are achieved respectively. Comparing with previous experiment results, the best classification rates involved Gabor filter increase 3.57%. The best performance is achieved with two optimal orientations $\pi/4$ and $\pi/2$. In general, the images with Gabor filter processing which involve frequency and orientation information could improve the best success rate.

CHAPTER 7

FUTURE SCOPE

For future studies more images from more dogs should be obtained. Here only 28 dogs with 14 normal and 14 abnormal were utilized In particular, more dogs in the abnormal class should be obtained. More images are necessary to have a higher degree of confidence in these results being a valid predictor of future performance.

The clinical application for such technique is being explored. The corresponding algorithms and features vectors will be used in pattern classification for the clinical experiment. The optimal feature combination from previous experiments will be used in the new pattern classification. The previous images are utilized as the fixed training set, and the new image is test set which will be classified with corresponding color normalization and feature vectors.

In addition, only the real part of the Gabor filter in this study was considered. Considering the real and imaginary parts of the complex form as a new image from which to obtain feature vectors may be helpful.

REFERENCES

André Ricardo Backes , Wesley Nunes Gonçalves , Alexandre Souto Martinez, Odemir Martinez Brunod, "Texture analysis and classification using deterministic tourist walk", Pattern Recognition 43 (2010), pg: 685 – 694.

Azmat, Z. Arkansas Valley Electr. Corp., AR,USA ; Turner, D.J. "Infrared thermography and its role in rural utility environment". Rural Electric Power Conference, 2005.

Anterior Cruciate Ligament; Wheeless' Textbook of Orthopaedics.

Barr, E S(1965), Infrared physics [0020-0891] vol:3 pg:195 -206.

CVIPtools (2010),"Computer Vision and Image processing Tools". http://cviptools.ece.siue.edu.

CVIP-FEPC (2010), "CVIP- Feature Extraction and Pattern Classification". http://cviptools.ece.siue.edu.

Daugman, J.G.: 'Uncertainty Relation for Resolution in Space, Spatial Frequency, and Orientation Optimized by Two-dimensional Visual Cortical Filters', J. Opt. Soc. Am. A, 1985, 2,47), pp. 1160-1169.

Fu H Freddie, Cohen Steven (2008), "Current Concepts in ACL Reconstruction" ISBN-13: 978-1556428135.

Gao JianBin ; Li Jian-Ping ; Xia Qi "Slowly Feature Analysis of Gabor Feature for Face Recognition" ICACIA 2008. pp: 177 – 180.

Grigorescu, S.E, Petkov, N. ; Kruizinga, P "Comparison of texture features based on Gabor filters" Image Processing, IEEE,2002, vol 11 pg:1160-1167.

Huysse WC, Verstraete KL. "Health Technology Assessment of Magnetic Resonance Imaging of the Knee." Eur J Radiol. Feb 2008;65(2):190-3.

Kruizinga P, Petkov and Grigorescu S.E " Comparison of Texture Features Based on Gabor filters", Proceedings of the 10th International Conference on Image Analysis and Processing, Venice, Italy, September 27-29, 1999, pp.142-147.

Lee C. J., and Wang S. D "Fingerprint Feature Extraction Using Gabor Filter", Electron. Lett., vol. 35, no. 4,Feb. 1999, pp. 288-290.

Lisowska-Lis A, Mitkowski S.A & Augustyn J, "Infrared Technique and Its Application in Science and Engineering in the Study Plans of Students in Electrical Engineering and Electronics" 2nd World Conference on Technology and Engineering Education Ljubljana, Slovenia, 5-8 September 2011.

Medical Imaging technique: http://en.wikipedia.org/wiki/Medical_imaging.

Wright, M(2012),"Knee Assessment", http://www.patient.co.uk/doctor/knee-assessment.

Muhammad Sha, Adeel K, Mudassar RAZA, Sajjad MOHSIN "Face Recognition using Gabor Filters" Journal of Applied Computer Science & Mathematics, no. 11 (5) /2011.

Naranje S, Mittal R, Nag H, Sharma R. "Arthroscopic and magnetic resonance imaging evaluation of meniscus lesions in the chronic anterior cruciate ligament-deficient knee. " Arthroscopy. Sep 2008;24(9):1045-51.

Pokorn´y J, Sn´aˇsel V, Richta K (Eds.), ″Shape Extraction Framework for Similarity Search in Image Databases", Dateso 2007, pp. 89–102, ISBN 80-7378-002-X.

Thermography technique website: URL: http://en.wikipedia.org/wiki/Thermography.

Umbaugh S. E (2010), “Digital Image Processing and Analysis: Human and Computer Vision Applications with CVIPtools, Second Edition”. The CRC Press, Boca Raton, FL, 2010.

Umbaugh S. E.“Digital Image Processing and Analysis: Human and Computer Vision Applications with CVIPtools, Third Edition”. The CRC Press, Boca Raton, FL, 2011

Umbaugh S. E, Solt P, “Veterinary thermographic image analysis.” Data and temperature normalization”. SIUE CVIP Laboratory report number 4878-3, January 23, 2008, unpublished.

Umbaugh S. E., Fu Jiyuan., Subedi Samrat. (May 2014),“Veterinary Thermographic Image Analysis”. Project Number 7-64878, Report Number 4878-25, May 13, 2013.

APPENDIX I

COMBINED COLOR NORMALIZATION RESULTS

In the appendix I, the results with combined color normalization operation of abnormal and normal groups.

Experimental Results

IMAGES and VIEWS (regions)
28 dogs total, 14 abnormal and 14 normal. The abnormal dogs have one abnormal side and one normal side.
Anterior stifle
Lateral stifle
Posterior stifle

CLASSIFICATION METHOD AND DISTANCE METRIC
K-Nearest Neighbor with K = 5 and NN, distance metric: Euclidean

FEATURES
Histogram features: Mean, Standard deviation, Skew, Energy and Entropy
Texture features: Energy, Inertia, Correlation, Inverse difference, and Entropy. The pixel distance was 6.
New texture functions are used.
Spectral Features was used with Rings = 3 and Sectors = 3.

DATA NORMALIZATION METHOD
Soft-max with r = 1
Standard Normal Density
None

METHOD
Leave One Out

OVERVIEW
15 sets of experiments were performed, including color normalization
5 group anterior stifle images
5 group lateral stifle images
5 group posterior stifle images
3 sets had 1023 permutations and 12 sets had 2047 permutations.

Anterior stifle Images Group:

For the first experiment (Anterior Stifle, Original for color normalization), 56 images include 42 Normal and 14 Abnormal).
For the second experiment (Anterior Stifle, Lum for color normalization), 56 images include 42 Normal and 14 Abnormal).
For the third experiment (Anterior Stifle, NormGrey for color normalization), 56 images include 42 Normal and 14 Abnormal).
For the fourth experiment (Anterior Stifle, NormRGB for color normalization), 56 images include 42 Normal and 14 Abnormal).
For the fifth experiment (Anterior Stifle, NormRGB-lum for color normalization), 56 images include 42 Normal and 14 Abnormal).

Lateral Stifle Image Group:

For the sixth experiment (Lateral Stifle, Original for color normalization), 56 images include 42 Normal and 14 Abnormal).
For the seventh experiment (Lateral Stifle, Lum for color normalization), 56 images include 42 Normal and 14 Abnormal).
For the eighth experiment (Lateral Stifle, NormGrey for color normalization), 56 images include 42 Normal and 14 Abnormal).
For the ninth experiment (Lateral Stifle, NormRGB for color normalization), 56 images include 42 Normal and 14 Abnormal).
For the tenth experiment (Lateral Stifle, NormRGB-lum for color normalization), 56 images include 42 Normal and 14 Abnormal).

Posterior Stifle Image Group:

For the eleventh experiment (Posterior Stifle, Original for color normalization), 56 images include 42 Normal and 14 Abnormal).
For the twelfth experiment (Posterior Stifle, Lum for color normalization), 56 images include 42 Normal and 14 Abnormal).
For the thirteenth experiment (Posterior Stifle, NormGrey for color normalization), 56 images include 42 Normal and 14 Abnormal).
For the fourteenth experiment (Posterior Stifle, NormRGB for color normalization), 56 images include 42 Normal and 14 Abnormal).
For the fifteenth experiment (Posterior Stifle, NormRGB-lum for color normalization), 56 images include 42 Normal and 14 Abnormal).

Result Overview

Anterior stifle Images Group:

- The best result of experiment with Anterior Stifle original for color normalization used is 78.57%.
- The best result of experiment with Anterior Stifle lum for color normalization used is 78.57%.
- The best result of experiment with Anterior Stifle normGrey for color normalization used is 78.57%.
- The best result of experiment with Anterior Stifle normRGB for color normalization used is 83.93%.
- The best result of experiment with Anterior Stifle for normRGB-lum color normalization used is 87.50%

Lateral stifle Images Group:

- The best result of experiment with Lateral Stifle original for color normalization used is 78.57%.
- The best result of experiment with Lateral Stifle lum for color normalization used is 78.57%.
- The best result of experiment with Lateral Stifle normGrey for color normalization used is 80.36%.
- The best result of experiment with Lateral Stifle normRGB for color normalization used is 83.93%.
- The best result of experiment with Lateral Stifle for normRGB-lum color normalization used is 85.71%

Posterior stifle Images Group:

- The best result of experiment with Posterior Stifle original for color normalization used is 82.14%.
- The best result of experiment with Posterior Stifle lum for color normalization used is 80.35%.
- The best result of experiment with Posterior Stifle normGrey for color normalization used is 78.57%.
- The best result of experiment with Posterior Stifle normRGB for color normalization used is 82.14%.
- The best result of experiment with Posterior Stifle for normRGB-lum color normalization used is 82.14%

Anterior Stifle Results:

Results from Experiment Set #1.(Anterior Stifle).

Color normalization: Original for color normalization
Images: Dog Gait Image
Classes: Normal and Abnormal.
Texture Function: texture2, Spectral Feature were used
K-Nearest Neighbor: KNN= 5 and NN

Note: for complete results see the Excel spreadsheet file Anterior Stifle Original Experiment.

Features (texture pixel dist=6)	Normalization method	Body Part	Number of images per class	Classification Success
Spectral Texture Inertia Texture Entropy (Experiment 656)	Soft-max, r = l	Anterior	42 Normal and 14Abnormal	78.57%.
Texture Entropy	None	Anterior	42 Normal and 14Abnormal	76.79%.
Texture InvDiff	None	Anterior	42 Normal and 14Abnormal	76.79%.

Highest success rate for this body part: Experiment 656(Soft-max, r = l)
Sensitivity: 14.29%
Specificity: 100.00%

Results from Experiment Set #2.(Anterior Stifle).

Color normalization: Lum for color normalization
Images: Dog Gait Image
Classes: Normal and Abnormal.
Texture Function: texture2, Spectral Feature were used
K-Nearest Neighbor: K = 5 and Nearest Neighbor

Features (texture pixel dist=6)	Normalization method	Body Part	Number of images per class	Classification Success
Histogram Skew (KNN=5)	Soft-max, r = l	Anterior	42 Normal and 14Abnormal	78.57%.
Texture Inertia Histogram Skew	Soft-max, r = l	Anterior	42 Normal and 14Abnormal	78.57%
Texture Inertia Histogram Skew	Standard Normal Density	Anterior	42 Normal and 14Abnormal	78.57%.

Highest success rate:
Sensitivity: 42.86%
Specificity: 90.48%

Results from Experiment Set #3.(Anterior Stifle).

Color normalization: NormGrey for color normalization
Images: Dog Gait Image
Classes: Normal and Abnormal.
Texture Function: texture2, Spectral Feature were used
K-Nearest Neighbor: K = 5 and Nearest Neighbor

Features (texture pixel dist=6)	Normalization method	Body Part	Number of images per class	Classification Success
Texture InvDiff Histogram Mean (NN)	Soft-max, r = l	Anterior	42 Normal and 14Abnormal	78.57%.
Texture Entropy	None	Anterior	42 Normal and 14Abnormal	76.79%
Texture InvDiff	None	Anterior	42 Normal and 14Abnormal	76.79%.

Highest success rate:
Sensitivity: 28.57%
Specificity: 97.62%

Results from Experiment Set #4.(Anterior Stifle).

Color normalization: NormRGB for color normalization
Images: Dog Gait Image
Classes: Normal and Abnormal.
Texture Function: texture2, Spectral Feature were used
K-Nearest Neighbor: K = 5 and Nearest Neighbor

Features (texture pixel dist=6)	Normalization method	Body Part	Number of images per class	Classification Success
Spectral Texture Inertia Texture InvDiff Histogram Entropy (NN)	Soft-max, r = 1	Anterior	42 Normal and 14Abnormal	83.93%.
Spectral Texture Inertia Histogram Mean Histogram StdDev Histogram Energy	Soft-max, r = 1	Anterior	42 Normal and 14Abnormal	83.93%.
Texture Correlation Histogram Energy	Soft-max, r = 1	Anterior	42 Normal and 14Abnormal	83.93%.

Highest success rate:
Sensitivity: 64.29%
Specificity: 90.48%

Results from Experiment Set #5.(Anterior Stifle).

Color normalization: NormRGB-lum for color normalization
Images: Dog Gait Image
Classes: Normal and Abnormal.
Texture Function: texture2, Spectral Feature were used
K-Nearest Neighbor: K = 5 and Nearest Neighbor

Features (texture pixel dist=6)	Normalization method	Body Part	Number of images per class	Classification Success	Classification algorithm
Spectral Texture Inertia Texture InvDiff Histogram StdDev Histogram Entropy (KNN=5)	Soft-max, r = l	Anterior	42 Normal and 14Abnormal	87.50%.	KNN=5
Spectral Texture Inertia Texture InvDiff Histogram Entropy	Soft-max, r = l	Anterior	42 Normal and 14Abnormal	85.71%	KNN=5
Spectral Texture InvDiff Histogram Skew Histogram Energy Histogram Entropy	Soft-max, r = l	Anterior	42 Normal and 14Abnormal	85.71%.	KNN=5

Highest success rate:
Sensitivity: 64.29%
Specificity: 95.24%

Lateral Stifle Results:

Results from Experiment Set #6.(Lateral Stifle).

Color normalization: Original for color normalization
Images: Dog Gait Image
Classes: Normal and Abnormal.
Texture Function: texture2, Spectral Feature were used
K-Nearest Neighbor: KNN= 5 and NN

Note: for complete results see the Excel spreadsheet file Lateral Stifle Original Experiment.

Features (texture pixel dist=6)	Normalization method	Body Part	Number of images per class	Classification Success
Spectral Texture InvDiff Histogram StdDev Histogram Entropy (Experiment 553)	Soft-max, r = l	Lateral	42 Normal and 14Abnormal	78.57%.
Spectral Texture InvDiff Histogram StdDev Histogram Skew Histogram Energy	Soft-max, r = l	Lateral	42 Normal and 14Abnormal	78.57%
Spectral Texture InvDiff Texture Entropy Histogram StdDev Histogram Entropy	Soft-max, r = l	Lateral	42 Normal and 14Abnormal	78.57%

Highest success rate for this body part: Experiment 553(Soft-max, r = l)
Sensitivity: 42.86%
Specificity: 90.48%

Results from Experiment Set #7.(Lateral Stifle).

Color normalization: Lum for color normalization
Images: Dog Gait Image
Classes: Normal and Abnormal.
Texture Function: texture2, Spectral Feature were used
K-Nearest Neighbor: K = 5 and Nearest Neighbor

Features (texture pixel dist=6)	Normalization method	Body Part	Number of images per class	Classification Success
Spectral Texture Energy Histogram StdDev (KNN=5)	Soft-max, r = l	Lateral	42 Normal and 14Abnormal	78.57%.
Texture Energy Texture Correlation Histogram StdDev Histogram Skew	Soft-max, r = l	Lateral	42 Normal and 14Abnormal	78.57%
Spectral Texture Energy Texture Entropy Histogram StdDev	Soft-max, r = l	Lateral	42 Normal and 14Abnormal	78.57%.

Highest success rate:
Sensitivity: 14.29%
Specificity: 100.00%

Results from Experiment Set #8.(Lateral Stifle).

Color normalization: NormGrey for color normalization
Images: Dog Gait Image
Classes: Normal and Abnormal.
Texture Function: texture2, Spectral Feature were used
K-Nearest Neighbor: K = 5 and Nearest Neighbor

Features (texture pixel dist=6)	Normalization method	Body Part	Number of images per class	Classification Success
Histogram Skew (KNN=5)	Soft-max, r = l	Lateral	42 Normal and 14Abnormal	80.36%.
Texture Inertia Histogram Skew	Soft-max, r = l	Lateral	42 Normal and 14Abnormal	80.36%
Texture Inertia Histogram Skew	Standard Normal Density	Lateral	42 Normal and 14Abnormal	80.36%.

Highest success rate:
Sensitivity: 28.57%
Specificity: 97.62%

Results from Experiment Set #9.(Lateral Stifle).

Color normalization: NormRGB for color normalization
Images: Dog Gait Image
Classes: Normal and Abnormal.
Texture Function: texture2, Spectral Feature were used
K-Nearest Neighbor: K = 5 and Nearest Neighbor

Features (texture pixel dist=6)	Normalization method	Body Part	Number of images per class	Classification Success
Texture Energy Texture Correlation Histogram Mean (NN)	Soft-max, r = l	Lateral	42 Normal and 14Abnormal	83.93%.
Histogram Mean Histogram StdDev Histogram Energy	Soft-max, r = l	Lateral	42 Normal and 14Abnormal	82.14%.
Texture Energy Texture Correlation Histogram Energy	Soft-max, r = l	Lateral	42 Normal and 14Abnormal	82.14%.

Highest success rate:
Sensitivity: 64.29%
Specificity: 90.48%

Results from Experiment Set #10.(Lateral Stifle).

Color normalization: NormRGB-lum for color normalization
Images: Dog Gait Image
Classes: Normal and Abnormal.
Texture Function: texture2, Spectral Feature were used
K-Nearest Neighbor: K = 5 and Nearest Neighbor

Features (texture pixel dist=6)	Normalization method	Body Part	Number of images per class	Classification Success
Texture Correlation Texture InvDiff Texture Entropy Histogram StdDev Histogram Skew Histogram Entropy (NN)	Soft-max, r = 1	Lateral	42 Normal and 14Abnormal	85.71%
Texture Energy Texture Correlation Texture InvDiff Histogram Skew	Soft-max, r = 1	Lateral	42 Normal and 14Abnormal	85.71%
Texture Energy Texture Correlation Texture InvDiff Texture Entropy Histogram Skew	Soft-max, r = 1	Lateral	42 Normal and 14Abnormal	85.71%.

Highest success rate:
Sensitivity: 64.29%
Specificity: 92.86%

Posterior Stifle Results:

Results from Experiment Set #11.(Posterior Stifle).

Color normalization: Original for color normalization
Images: Dog Gait Image
Classes: Normal and Abnormal.
Texture Function: texture2, Spectral Feature were used
K-Nearest Neighbor: KNN= 5 and NN

Note: for complete results see the Excel spreadsheet file Posterior Stifle Original Experiment.

Features (texture pixel dist=6)	Normalization method	Body Part	Number of images per class	Classification Success
Texture Energy Texture InvDiff Texture Entropy Histogram StdDev Histogram Skew (Experiment 316)	Soft-max, r = l	Posterior	42 Normal and 14Abnormal	82.14%
Texture InvDiff Texture Entropy Histogram Entropy	Soft-max, r = l	Posterior	42 Normal and 14Abnormal	80.35%
Texture Energy Texture InvDiff Histogram StdDev	Soft-max, r = l	Posterior	42 Normal and 14Abnormal	80.35%

Highest success rate: Experiment 316(Soft-max, r = l)
Sensitivity: 35.71%
Specificity: 97.62%

Results from Experiment Set #12.(Posterior Stifle).

Color normalization: Lum for color normalization
Images: Dog Gait Image
Classes: Normal and Abnormal.
Texture Function: texture2, Spectral Feature were used
K-Nearest Neighbor: K = 5 and Nearest Neighbor

Features (texture pixel dist=6)	Normalization method	Body Part	Number of images per class	Classification Success
Texture Entropy Histogram Mean (KNN=5)	Soft-max, r = l	Posterior	42 Normal and 14Abnormal	80.35%.
Spectral Histogram Mean Histogram Entropy	Soft-max, r = l	Posterior	42 Normal and 14Abnormal	80.35%
Texture InvDiff Texture Entropy Histogram Mean	Soft-max, r = l	Posterior	42 Normal and 14Abnormal	80.35%.

Highest success rate:
Sensitivity: 28.57%
Specificity: 97.62%

Results from Experiment Set #13.(Posterior Stifle).

Color normalization: NormGrey for color normalization
Images: Dog Gait Image
Classes: Normal and Abnormal.
Texture Function: texture2, Spectral Feature were used
K-Nearest Neighbor: K = 5 and Nearest Neighbor

Features (texture pixel dist=6)	Normalization method	Body Part	Number of images per class	Classification Success
Texture InvDiff (KNN=5)	None	Posterior	42 Normal and 14Abnormal	78.57%.
Texture Inertia Texture InvDiff Histogram Skew Histogram Entropy	Soft-max, r = l	Posterior	42 Normal and 14Abnormal	76.79%.
Spectral Texture Entropy Histogram Entropy	Standard Normal Density	Posterior	42 Normal and 14Abnormal	76.79%.

Highest success rate:
Sensitivity: 28.57%
Specificity: 95.24%

Results from Experiment Set #14.(Posterior Stifle).

Color normalization: NormRGB for color normalization
Images: Dog Gait Image
Classes: Normal and Abnormal.
Texture Function: texture2, Spectral Feature were used
K-Nearest Neighbor: K = 5 and Nearest Neighbor

Features (texture pixel dist=6)	Normalization method	Body Part	Number of images per class	Classification Success
Spectral Texture Inertia Histogram StdDev Histogram Skew Histogram Energy	Soft-max, r = 1	Posterior	42 Normal and 14Abnormal	82.14%.
Spectral Texture Inertia Histogram Mean Histogram StdDev Histogram Skew Histogram Energy	Soft-max, r = 1	Posterior	42 Normal and 14Abnormal	82.14%.
Spectral Texture Correlation Texture Entropy	Soft-max, r = 1	Posterior	42 Normal and 14Abnormal	80.35%.

Highest success rate:
Sensitivity: 35.71%
Specificity: 97.62%

Results from Experiment Set #15.(Posterior Stifle).

Color normalization: NormRGB-lum for color normalization
Images: Dog Gait Image
Classes: Normal and Abnormal.
Texture Function: texture2, Spectral Feature were used
K-Nearest Neighbor: K = 5 and Nearest Neighbor

Features (texture pixel dist=6)	Normalization method	Body Part	Number of images per class	Classification Success
Texture Energy Texture Inertia Texture InvDiff Histogram Mean Histogram Energy (NN)	Soft-max, r = 1	Posterior	42 Normal and 14Abnormal	82.14%.
Texture InvDiff Texture Entropy Histogram StdDev	Soft-max, r = 1	Posterior	42 Normal and 14Abnormal	80.35%
Texture Correlation Histogram Mean Histogram Entropy	Soft-max, r = 1	Posterior	42 Normal and 14Abnormal	80.35%.

Highest success rate:
Sensitivity: 28.57%
Specificity: 100.00%